



## Germline but macrophage-tropic CYBB mutations in kindreds with X-linked predisposition to tuberculous mycobacterial diseases

Jean-Laurent Casanova, Jacinta Bustamante, Andres Augusto Arias, Guillaume Vogt, Capucine Picard, Lizbeth Blancas Galicia, Carolina Prando, Audrey Grant, Christophe Marchal, Marjorie Hubeau, et al.

### ► To cite this version:

Jean-Laurent Casanova, Jacinta Bustamante, Andres Augusto Arias, Guillaume Vogt, Capucine Picard, et al.. Germline but macrophage-tropic CYBB mutations in kindreds with X-linked predisposition to tuberculous mycobacterial diseases. *Nature Immunology*, 2011, 10.1038/ni.1992 . hal-00612702

**HAL Id: hal-00612702**

**<https://hal.science/hal-00612702>**

Submitted on 30 Jul 2011

**HAL** is a multi-disciplinary open access archive for the deposit and dissemination of scientific research documents, whether they are published or not. The documents may come from teaching and research institutions in France or abroad, or from public or private research centers.

L'archive ouverte pluridisciplinaire **HAL**, est destinée au dépôt et à la diffusion de documents scientifiques de niveau recherche, publiés ou non, émanant des établissements d'enseignement et de recherche français ou étrangers, des laboratoires publics ou privés.

**Germline but macrophage-tropic *CYBB* mutations  
in kindreds with X-linked predisposition to tuberculous mycobacterial diseases**

Jacinta Bustamante<sup>1,2</sup>, Andres A. Arias<sup>3,\*</sup>, Guillaume Vogt<sup>4,\*</sup>, Capucine Picard<sup>1,2,5,6,\*</sup>,  
Lizbeth Blancas Galicia<sup>1,2,7</sup>, Carolina Prando<sup>4</sup>, Audrey V. Grant<sup>1,2</sup>, Christophe C. Marchal<sup>3</sup>,  
Marjorie Hubeau<sup>1,2</sup>, Ariane Chappier<sup>1,2</sup>, Ludovic de Beaucoudrey<sup>1,2</sup>, Anne Puel<sup>1,2</sup>,  
Jacqueline Feinberg<sup>1,2</sup>, Ethan Valinetz<sup>3</sup>, Lucile Jannière<sup>1,2</sup>, Céline Besse<sup>8</sup>, Anne Boland<sup>8</sup>,  
Jean-Marie Brisseau<sup>9</sup>, Stéphane Blanche<sup>6</sup>, Olivier Lortholary<sup>10</sup>, Claire Fieschi<sup>1,2,11</sup>,  
Jean-François Emile<sup>12</sup>, Stéphanie Boisson-Dupuis<sup>1,2,4</sup>, Saleh Al-Muhsen<sup>13</sup>,  
Bruce Woda<sup>14\*\*</sup>, Peter E. Newburger<sup>15\*\*</sup>, Antonio Condino-Neto<sup>16\*\*</sup>,  
Mary C. Dinauer<sup>3\*\*</sup>, Laurent Abel<sup>1,2,4</sup> and Jean-Laurent Casanova<sup>1,2,4,6,13</sup>

*Address all correspondence to Jean-Laurent Casanova, MD, PhD,  
Laboratory of Human Genetics of Infectious Diseases, Rockefeller Branch,  
The Rockefeller University, 1230 York Avenue, New York, NY 10065, USA  
Tel 1 212 327 7331; Fax 1 212 327 7330; E-mail [jean-laurent.casanova@rockefeller.edu](mailto:jean-laurent.casanova@rockefeller.edu)*

1. Laboratory of Human Genetics of Infectious Diseases, Necker Branch, Institut National de la Santé et de la Recherche Médicale, U980, 75015 Paris, France, EU
2. Paris Descartes University, Necker Medical School, 75015 Paris, France, EU
3. Wells Center for Pediatric Research, Department of Pediatrics, Indiana University School of Medicine, Indianapolis, IN 46202, USA
4. St. Giles Laboratory of Human Genetics of Infectious Diseases, Rockefeller Branch, The Rockefeller University, New York, NY 10065, USA
5. Center for the Study of Primary Immunodeficiencies, AP-HP, Necker Hospital, 75015 Paris, France, EU
6. Pediatric Hematology-Immunology Unit, Necker Hospital, AP-HP, 75015 Paris, France, EU
7. National Institute of Pediatrics, Unit of Immunodeficiency, 3700 Mexico City, Mexico
8. National Genotyping Center, 91057 Evry, France, EU
9. Department of Internal Medicine, Nantes Hospital, 44000 Nantes, France, EU
10. Department of Infectious Diseases, AP-HP, Necker Hospital, 75015 Paris, France, EU
11. Adult Immunopathology Unit, Saint Louis Hospital, 75010 Paris, France, EU
12. Department of Pathology, Institut National de la Santé et de la Recherche Médicale, U602, Ambroise Paré Hospital and Versailles Saint-Quentin-en-Yvelines University, 92100 Boulogne, France, EU
13. Prince Naif Center for Immunology Research, Department of Pediatrics, College of Medicine, King Saud University, Riyadh, Saudi Arabia
14. Department of Pathology, University of Massachusetts Medical School, Worcester, MA 01655, USA
15. Departments of Pediatrics and Cancer Biology, University of Massachusetts Medical School Worcester, MA 01655, USA
16. Department of Immunology, Institute of Biomedical Sciences, University of São Paulo, 05508-000 São Paulo, SP, Brazil

\* and \*\*: equal contributions

**Abstract**

Germline mutations in the human *CYBB* gene, encoding the gp91<sup>phox</sup> subunit of the phagocyte NADPH oxidase, impair the respiratory burst of all types of phagocytes and result in X-linked chronic granulomatous disease. We report two kindreds in which otherwise healthy male adults show X-linked recessive Mendelian susceptibility to mycobacterial diseases. These patients harbor novel mutations in *CYBB* that profoundly reduce the respiratory burst in monocyte-derived macrophages, but not in monocytes or granulocytes. The macrophage-specific functional consequences of the germline mutation result from the cell-specific impairment of NADPH oxidase assembly. This “experiment of nature” indicates that *CYBB* is a Mendelian mycobacterial susceptibility gene and demonstrates that the respiratory burst in human macrophages is a crucial mechanism for protective immunity to tuberculous mycobacteria.

**Key words:** tuberculosis, BCG vaccine, macrophages, NADPH activity.

Tuberculosis is a leading public health problem worldwide and the study of genetic predisposition to tuberculosis is a promising avenue of research<sup>1,2</sup>. Mendelian susceptibility to mycobacterial disease (MSMD; MIM 209950) is a rare syndrome, resulting in predisposition to clinical disease caused by weakly virulent mycobacterial species, such as tuberculous *Mycobacterium bovis* Bacillus Calmette-Guérin (BCG) vaccines and non-tuberculous, environmental mycobacteria<sup>1,3</sup>. These patients are also vulnerable to more virulent *M. tuberculosis*<sup>2</sup>. Five disease-causing autosomal genes (*IFNGR1*, *IFNGR2*, *STAT1*, *IL12RB1* and *IL12B*) and one X-linked gene (*NEMO*) have been found<sup>3</sup>. Allelic heterogeneity accounts for the existence of 13 distinct disorders, all of which impair IFN- $\gamma$ -mediated immunity. The genetic etiology of about half of the patients with MSMD however remains unclear. We previously reported four maternally related French male patients (kindred A, P1 to P4) presenting a second X-linked recessive form of MSMD<sup>4</sup> (XR-MSMD-2) (**Fig. 1a**). The patients had recurrent or disseminated tuberculous mycobacterial disease: BCG-disease in three patients (MSMD *sensu stricto*) and tuberculosis in one (not vaccinated by BCG). We recently identified another French kindred with XR-MSMD; the three male patients of this kindred (kindred B, P5 to P7) had BCG-disease. In patients from both kindreds, there was no distinguishable immunological phenotype and the known etiologies of MSMD, including, in particular, mutations in X-linked *NEMO*<sup>5</sup>, were excluded, suggesting that the two kindreds may share a new XR genetic etiology of MSMD.

## Results

### *CYBB* mutations associated with MSMD

Multipoint linkage analysis in the two kindreds (**Methods** and **Supplementary information**) gave a maximal LOD score of 2.29 for two candidate regions on Xp11.3-Xp21.1 (13.83 Mb) and Xq25-Xq26.3 (11.79 Mb) (**Supplementary Fig. 1a**). Known X-linked primary immunodeficiencies (PIDs) were previously excluded on clinical and immunological grounds in both kindreds. We nonetheless sequenced the coding region of the PID-causing genes present in these two chromosomal intervals, using DNA isolated from the two probands (P4 in kindred A and P5 in kindred B). No mutations were found in *TNFSF5*, encoding CD40L (CD154)<sup>6</sup> but a nucleotide substitution (A->C) in the codon for amino acid position 231, resulting in the replacement of a glutamine by a proline residue (Q231P), was found in exon 7 of *CYBB* in P4 from kindred A (**Fig. 1a** and **b**). A nucleotide substitution (A->C) in the codon for amino acid position 178, resulting in the replacement of a threonine by a proline residue (T178P), was found in exon 6 of *CYBB* in P5 from kindred B (**Fig. 1a** and **b**). Mutations of *CYBB* are commonly associated with chronic granulomatous disease (CGD)<sup>7</sup>. In both kindreds, the clinically affected male subjects were all hemizygous for the mutant allele, whereas the other maternally related, healthy male subjects tested were not. The eleven obligate female carriers tested in the two kindreds were heterozygous, including an 90-year-old woman with a history of severe tuberculosis (H1), as well as four other female subjects (**Fig. 1a**). The strict familial co-segregation of the *CYBB* genotype and the MSMD phenotype (extended to tuberculosis) in the male subjects alive from both kindreds suggested that the *CYBB* mutations were responsible for disease. The mutations must have been transmitted by the male founders of both kindreds in generation I, although they did not display MSMD (**Fig. 1a**). These men however lived in France before the introduction of routine BCG vaccination in children, at a time at which tuberculosis

was already declining. The Q231P and T178P *CYBB* alleles were not found in any of 1,300 X chromosomes from 52 ethnic groups (in the HGDP-CEPH panel), including 240 European chromosomes. Moreover, the two mutations are non-conservative, both substituting a Proline which is particularly disruptive (**Fig. 1c**), and affect residues that are conserved in the 33 animal species studied (**Supplementary Fig. 1b**). Finally, these two mutations have not previously been associated with CGD, a well known PID which is associated with multiple bacterial and fungal infectious diseases, including tuberculous mycobacterial diseases<sup>7-13</sup> (**Supplementary information**). All these observations are thus consistent with the Q231P and T178P *CYBB* mutations being responsible for XR-MSMD-2 in these two kindreds.

#### **Normal NADPH oxidase activity in circulating phagocytes**

*CYBB* encodes the  $\beta$  chain of flavocytochrome-b<sub>558</sub>, also known as gp91<sup>phox</sup> or NOX2, an essential element of the nicotinamide adenine dinucleotide phosphate (NADPH) oxidase complex (PHOX) in phagocytes, such as granulocytes, monocytes, and macrophages. It is also expressed, but to a lesser extent, in other cells, such as dendritic cells and B lymphocytes. In all phagocytes of patients with CGD or “variant CGD”, the production of reactive oxygen species (ROS) is inadequate. To solve the paradox of *CYBB* mutations in two kindreds with MSMD but apparently not CGD or “variant CGD” (**Supplementary information**), we therefore investigated in depth the respiratory burst in our patients bearing the Q231P or T178P *CYBB* mutation. P4 displayed normal O<sub>2</sub><sup>-</sup> and H<sub>2</sub>O<sub>2</sub> production in polymorphonuclear neutrophils (PMNs), as revealed by the reduction of nitroblue tetrazolium (NBT) in response to endotoxin (LPS) and *Staphylococcus epidermidis* (data not shown and <sup>4</sup>). Moreover, the chemiluminescence of PMNs (a marker of both O<sub>2</sub><sup>-</sup> and H<sub>2</sub>O<sub>2</sub> concentrations) stimulated with 4-beta-phorbol 12-beta-myristate 13-alpha-acetate (PMA) was also normal<sup>4</sup>. O<sub>2</sub><sup>-</sup> production in PMNs from the five patients tested,

stimulated with PMA in the presence or absence of catalase, was assessed by superoxide dismutase-inhibitable cytochrome-*c* reduction (a specific method for  $O_2^-$  determination).  $O_2^-$  production was in the normal range, even at early time points, and proportional to the number of PMNs tested, even in the presence of catalase (**Fig. 2a** and **Supplementary Fig. 2a** and **2b**). PMNs from the six patients tested also released  $H_2O_2$  normally in response to PMA<sup>14</sup> (**Fig. 2b** and **Supplementary Fig. 2c**). Following PMA treatment  $O_2^-$ -dependent cytochrome-*c* reduction in monocytes from the six patients tested was normal (**Fig. 2a** and **Supplementary Fig. 2d** and **2e**). Similar amounts of  $H_2O_2$  were released after PMA activation of the monocytes from the five patients tested and healthy controls, contrasting with the defect seen in monocytes from CGD patients (**Fig. 2b** and **Supplementary Fig. 2f**). PMNs and monocytes from four heterozygous female subjects responded like control cells (**Supplementary Fig. 2f**). In addition, functional respiratory burst activity was assessed by flow cytometry, using dihydrorhodamine 123 (DHR) to measure intracellular levels of  $H_2O_2$  production. PMNs and monocytes from P4 (kindred A) and P5 (kindred B) stimulated with PMA were normal (**Fig. 2c** and **Supplementary Fig. 2g**). Moreover, PMNs from P4 and P5 responded normally to milder activation involving priming with low concentrations of TNF, IL-1 $\beta$  or cytochalasin b, followed by fMLF stimulation (**Fig. 2d** and **Supplementary Fig. 2h**). Thus, blood PMNs and monocytes from the six patients bearing the Q231P or T178P *CYBB* allele tested showed a normal respiratory burst in peripheral blood PMNs and monocytes, as assessed by diverse assays of  $O_2^-$  production and  $H_2O_2$  release. Finally, we searched for subtle functional defects that might have been missed by the previous experiments, by evaluating the *in vitro* killing of *Staphylococcus aureus* by granulocytes from one patient from each kindred. Their granulocytes killed *S. aureus* normally, unlike granulocytes from patients with CGD, in which *S. aureus* is the leading pathogen (**Fig. 2e**). These findings

confirm previous investigations of these patients' respiratory burst<sup>4</sup> and are consistent with the absence of clinical features typically associated with CGD and "variant CGD", including staphylococcal disease, even in affected adults of advanced age from kindreds A and B (**Fig. 1a**)<sup>4</sup>.

### **Impaired NADPH oxidase activity in macrophages**

In turn, these findings raised the question of whether the two *CYBB* alleles were pathogenic at all in the two kindreds with MSMD. We thus investigated the cellular basis of mycobacterial disease in these patients by assessing the oxidative function of their monocyte-derived macrophages (MDMs)<sup>15,16</sup>. Indeed, tissue phagocytes, macrophages in particular, are the natural hosts of mycobacteria in the course of infection and disease. After 14 to 15 days of culture in the presence of M-CSF to generate MDMs, H<sub>2</sub>O<sub>2</sub> was clearly detectable when control MDMs were cultured for 16 to 18 hours with live BCG or PPD (purified protein derivative from *M. tuberculosis*) before PMA stimulation (**Supplementary Fig. 3a**). In the same conditions, macrophages from CGD patients, P1, P2, P3, and P4 (Q231P, kindred A), released no detectable H<sub>2</sub>O<sub>2</sub>. In similar conditions, but using interferon- $\gamma$  (IFN- $\gamma$ ) rather than BCG or PPD, Q231P macrophages also did not respond normally to the PMA trigger (**Supplementary Fig. 3a**). M-CSF-differentiated macrophages from P5 (T178P, kindred B) displayed a milder phenotype, as they released low, or in some conditions normal amounts of H<sub>2</sub>O<sub>2</sub> (**Supplementary Fig. 3a**). We also studied formazan granule deposition due to the reduction of NBT, as a sensitive indicator of O<sub>2</sub><sup>-</sup> production in individual macrophages derived from M-CSF-cultured monocytes. Only a very small fraction of BCG- or PPD-activated and PMA-triggered macrophages (less than 5%) from the four patients bearing the Q231P allele reduced NBT (**Supplementary Fig. 3b**). A larger



fraction of macrophages from P5 bearing the T178P allele reduced NBT, but were strongly positive in less than 50%. As tissue macrophages from the patients were not available, we next tested MDMs derived *in vitro* in two conditions thought to reflect *in vivo* differentiation. We cultured MDMs with M-CSF alone for 7 days, and added LPS plus IFN- $\gamma$  or IL-4. After 14 to 15 days of culture, MDMs (in any culture condition) from both P4 (kindred A) and P5 (kindred B) were unable to release detectable H<sub>2</sub>O<sub>2</sub>, in contrast to control cells (**Fig. 3**, and **Supplementary Fig. 3c**). Thus, unlike blood granulocytes and monocytes, MDMs bearing the Q231P or the T178P *CYBB* allele, in multiple conditions of *in vitro* differentiation and conditions of stimulation, showed impairment of the respiratory burst, which was almost abolished for Q231P and severely impaired for T178P. We could not test the respiratory burst of the patients' macrophages *in vivo* or *ex vivo*. We characterized the patients' macrophage defect further, by assessing the growth of BCG within MDMs derived *in vitro* from two patients (P4 and P6) and ten healthy controls. As assessed by counting CFU, the patients' MDMs controlled BCG significantly less well than control MDMs on day 14 ( $p=0.06$ ), and this difference was even more marked on day 21 ( $p=0.003$ ) (**Supplementary information** and **Supplementary Fig. 4**). No such difference was observed in the presence of exogenous IFN- $\gamma$ . These data provide a plausible mechanism for the co-segregation of the patients' *CYBB* mutation, their macrophage respiratory burst defect and their mycobacterial disease. As mycobacteria reside within macrophages *in vivo*, our *in vitro* experiments showing that MDMs in patients from each of the two kindreds display impairment of both the respiratory burst and of the control of BCG growth provide a plausible cellular basis for the occurrence of mycobacterial diseases in patients with XR-MSMD-2.

#### **Impaired NADPH oxidase activity in EBV-B cells**

208 *CYBB* is expressed in some B cells. Although irrelevant to the pathogenesis of XR-  
 209 MSMD-2, as B cell-deficient patients are not prone to mycobacterial diseases<sup>17,18</sup>, we made use  
 210 of this property to try to characterize the effects of the mutant *CYBB* alleles in Epstein Barr Virus  
 211 (EBV)-transformed B-cell lines (EBV-B cells)<sup>19</sup>. Upon activation with PMA, EBV-B cells from  
 212 22 unrelated healthy individuals and nine male members of kindred A not carrying the Q231P  
 213 *CYBB* mutation were capable of producing O<sub>2</sub><sup>-</sup> (**Fig. 4a** and **Supplementary Fig. 5**). However,  
 214 EBV-B cells from kindreds A and B (P1 to P7), like cells from XR-CGD patients, produced no  
 215 detectable O<sub>2</sub> (**Fig. 4a** and **Supplementary Fig. 5**). We then measured the release of H<sub>2</sub>O<sub>2</sub> by  
 216 EBV-B cells from P1 to P7 upon stimulation with various concentrations of PMA for various  
 217 periods of time. None of the EBV-B cells from the seven patients released any detectable H<sub>2</sub>O<sub>2</sub>,  
 218 like XR-CGD patients (**Fig. 4b**). Only 1 to 3% of the cells from the patients (P1 to P7) reduced  
 219 NBT to formazan upon activation with PMA (**Fig. 4c**). EBV-B cells, MDMs therefore shared a  
 220 similar cellular phenotype. We transiently transfected EBV-B cells from a healthy control, a  
 221 patient with XR-CGD, P4 (kindred A), or P5 (kindred B) with plasmid-encoded wild-type or  
 222 mutant *CYBB*, to determine whether the Q231P and T178P alleles were functionally  
 223 hypomorphic. We then assessed the functional reconstitution of the respiratory burst in assays of  
 224 NBT reduction. Forty-eight hours after transfection with wild-type *CYBB*, 10 to 13% of the cells  
 225 from a patient with XR-CGD, P4, or P5 reduced NBT, but neither mock transfection nor  
 226 transfection with either mutant *CYBB* had this effect (data not shown). We also established stable  
 227 transfectants by means of a retroviral vector, and quantified the respiratory burst by assessing  
 228 H<sub>2</sub>O<sub>2</sub> release. Stable transfection with WT *CYBB* allele complemented the defect in Q231P,  
 229 T178P EBV-B cells indicating the restoration of a functional respiratory burst in Q231P, T178P  
 230 and XR-CGD EBV-B cells transduced with wild-type *CYBB* (**Fig. 4d**); however, no  
 231 complementation of the cellular phenotype (no detectable respiratory burst) was observed after

transduction of XR-CGD cells transduced with the Q231P or T178P allele (**Fig. 4d**). Thus, EBV-B cells from these patients had an impaired respiratory burst because they carried the Q231P or T178P *CYBB* allele. A lack of respiratory burst in peripheral B cells, by inference from EBV-B cells, would not account for MSMD<sup>17,18</sup>, but we demonstrate a causal relationship between two mutants hemizygous for Q231P or T178P *CYBB* mutations and impairment of the respiratory burst likely also applies to the patients' MDMs (M-CSF + IL4) (e.g. **Fig. 3**), which could account for the clinical phenotype of MSMD. In contrast, these *CYBB* alleles did not impair the respiratory burst of PMNs or monocytes (**Fig. 2** and **Supplementary Fig. 2**), explaining the lack of the CGD or "variant CGD" phenotype in the patients.

#### **Impaired gp91<sup>phox</sup> expression in macrophages**

The observed impairment of the functional respiratory burst in the patients' EBV-B cells and MDMs but not in PMNs or monocytes was investigated. The amount of *CYBB* mRNA was determined by real-time RT-PCR in four cell types from the five patients from two kindreds tested and was found to be similar to that in 5\_healthy controls (**Supplementary Fig. 6a** and **6b**). We next investigated the cell-specific impact of the germline Q231P and T178P *CYBB* mutations by assessing gp91<sup>phox</sup> expression in the corresponding cells by immunoblotting with three specific antibodies (recognizing different epitopes on the gp91<sup>phox</sup> protein) and increasing amounts of proteins. PMNs produced the mutant protein Q231P gp91<sup>phox</sup> in diminished but detectable amounts (**Fig. 5a**, **Supplementary Fig. 6c**). Experiments with the antibody 54.1 suggested that PMNs produced almost normal amounts of T178P gp91<sup>phox</sup>, whereas experiments with the other two antibodies suggested that this protein was produced in smaller amounts, perhaps reflecting the nature of the epitopes recognized (**Fig. 5a** and **Supplementary Fig. 6c**). Mutant Q231P protein levels were similarly low in monocytes, in which mutant T178P protein levels were also

reduced but less affected (**Fig. 5a, 5b**). Interestingly, the gp91<sup>phox</sup> protein expression defect for the Q231P and T178P mutant gp91<sup>phox</sup> was much more pronounced in MDMs (**Fig. 5b**), correlating with the greater defect in the respiratory burst in this cell type (**Fig. 3** and **Supplementary Fig. 3**). However, a species migrating at 65 kDa was detected in the Q231P and T178P macrophage samples (**Fig. 5b**). This size corresponds to the high mannose gp65 precursor of gp91<sup>phox</sup>, which may be more stable in macrophages compared to monocytes or macrophages, as has previously been reported for EBV-B cells<sup>20,21</sup>. This species is normally only transiently present in the endoplasmic reticulum prior to heme incorporation and heterodimer formation with p22<sup>phox</sup>, which is followed by additional carbohydrate processing of the CYBB subunit in the Golgi to the mature gp91<sup>phox</sup> of  $\approx$  91 kDa and ultimate targeting of flavocytochrome-b<sub>558</sub> to post-biosynthetic membrane compartments<sup>22-26</sup>. The gp65 species was also detected in an XR-CGD patient (**Fig. 5b**) with an L365P mutation in the flavin binding domain, but lacks gp91<sup>phox</sup> expression and neutrophil oxidase activity<sup>27</sup>. The presence of the gp65 intermediate suggests that these alleles are associated with impaired formation of the flavocytochrome b heterodimer, which is required for maturation of gp65 to gp91<sup>phox</sup>. Finally, we did not have access to fresh tissue macrophages, but assessed gp91<sup>phox</sup> production in the macrophages present in lymph node biopsy samples from two patients by immunohistochemistry (**Supplementary Fig. 6d** and **6e**). Impaired gp91<sup>phox</sup> production was seen in macrophages from P4 (Q231P), as in lymph nodes from CGD patients, but not in healthy controls. Residual gp91<sup>phox</sup> production was detected in tissue PMNs from P4. As expected, gp91<sup>phox</sup> was detected in both PMNs and macrophages from P5 (T178P). Altogether, these data indicate that the patients' defect of gp91<sup>phox</sup> expression is more pronounced in macrophages compared to neutrophils and monocytes, and overall more severe for the Q231P *CYBB* allele.

### Impaired gp91<sup>phox</sup> expression in EBV-B cells

We also tested EBV-B cells from a healthy control, XR-CGD (in this case, carrying a complete deletion of the *CYBB* allele), and the Q231P and T178P patients, and the same cells transduced by wild-type or one of the mutant *CYBB* alleles (**Fig. 5c**). Clearly, the two mutant *CYBB* alleles are poorly expressed in EBV-B cells, in which the 91 kDa form of gp91<sup>phox</sup> was barely detectable in cells derived from patients or following transduction of XR-CGD cells with retroviral vectors for expression of the mutant *CYBB* alleles. Again, a 65 kDa species corresponding to the high mannose precursor of the mature 91 kDa form of gp91<sup>phox</sup> was detected for each of the Q231P and T178P mutant alleles, in contrast to EBV-B cells from an XR-CGD patient with a large deletion encompassing the *CYBB* gene (**Fig. 5c**). We also investigated the expression of the other components of the NADPH oxidase complex. Levels of p22<sup>phox</sup> (which is encoded by *CYBA* and is normally bound to gp91<sup>phox</sup>) were reduced in PMNs and EBV-B cells, particularly in cells with the Q231P allele, paralleling gp91<sup>phox</sup> expression (**Supplementary Fig. 6f**). Although expression of p22<sup>phox</sup> in EBV-B cells is less affected by low or absent gp91<sup>phox</sup>, p22<sup>phox</sup> levels were still modestly reduced in EBV-B cells from P4 and P5 (**Supplementary Fig. 6g**) (providing further, indirect evidence for impaired gp91<sup>phox</sup> expression in the patients' EBV-B cells). The p47<sup>phox</sup> and p67<sup>phox</sup> subunits were normally expressed in patients' PMNs and EBV-B cells (**Supplementary Fig. 6f and 6g**). Reproducible differences in gp91<sup>phox</sup> protein abundance were observed between cell types in six patients carrying either Q231P or T178P, with less gp91<sup>phox</sup> in MDMs and EBV-B cells than in the patients' monocytes and PMNs, or as compared to in phagocytes and EBV-B cells from five controls. The Q231P *CYBB* mutation decreases the expression of the gp91<sup>phox</sup> protein *in vivo*, *ex vivo*, and *in vitro*, in granulocytes, monocytes, macrophages and EBV-B cells, with steady-state levels of this protein being determined in part by the cell type, with a more pronounced impact in macrophages and EBV-B cells. The 178P

gp91<sup>phox</sup> protein is expressed at higher levels but follows an identical pattern according to the cell type. These expression data are consistent with the normal functional respiratory burst in the patients' PMNs and monocytes, contrasting with the functional defect in oxidant production by EBV-B cells and MDMs.

### **Impaired expression of flavocytochrome-b<sub>558</sub>**

We then analyzed the cell surface expression of the flavocytochrome-b<sub>558</sub> complex (gp91<sup>phox</sup> and p22<sup>phox</sup>) on the plasma membrane by flow cytometry, using the monoclonal antibody 7D5, which recognizes residues <sup>160</sup>IKNP<sup>163</sup> and <sup>226</sup>RIVRG<sup>230</sup> on gp91<sup>phox</sup> in the presence of p22<sup>phox</sup><sup>29,30</sup>. Cell surface flavocytochrome-b<sub>558</sub> was clearly detectable in PMNs and monocytes from the two patients tested here, from two different kindreds, although at reduced levels for the Q231P allele (**Fig. 5d** and **Supplementary Fig. 6h**). By contrast, flavocytochrome-b<sub>558</sub> was barely detectable on EBV-B cells from seven patients tested among both kindreds (**Fig. 5e**). Identical results were obtained by spectrophotometric measurements of reduced minus oxidized difference absorption spectra for PMNs and EBV-B cells (**Supplementary Fig. 6i**). Adherent MDMs were not suitable for these two assays and we did not have access to fresh tissue macrophages. Analysis of the cell surface expression of flavocytochrome-b<sub>558</sub> in PMNs, monocytes and EBV-B cells from the heterozygous female subjects revealed the presence of two discrete cell populations — those expressing and those not expressing flavocytochrome-b<sub>558</sub> — correlating with both the functional respiratory burst and the inactivated X chromosome (**Supplementary Fig. 7a** and **7b**, and **Supplementary information**). Similar findings were obtained in NBT assays on MDMs from heterozygous female subjects (**Supplementary Fig. 7c**). Thus, the Q231P and T178P mutations impair NADPH oxidase gp91<sup>phox</sup> expression to a greater extent in MDMs and EBV-B cells than in PMNs and monocytes, revealing a profound cell type-

specific effect on the flavocytochrome-b<sub>558</sub> complex, in terms of both surface and total expression. The relatively greater impact of the mutant alleles in MDMs and EBV-B cells may reflect cell-type-related differences in production of flavocytochrome-b<sub>558</sub>, which is higher in PMNs and monocytes compared to MDMs and EBV-B cells<sup>31,19</sup>. The much smaller amounts of mutant gp91<sup>phox</sup> protein produced in EBV-B cells and in MDMs, and possibly in tissue macrophages, severely limit the capacity for the assembly of a functional NADPH oxidase complex, whereas the amounts produced in PMNs and monocytes, although smaller than normal, particularly for the Q213P allele, are sufficient to support assembly of adequate amounts of the functional enzyme complex to produce oxidants at normal levels (**Fig. 2**)<sup>32-35</sup>. Taken together, cell-type differences in the level of production of gp91<sup>phox</sup> and the assembly of the flavocytochrome-b<sub>558</sub> heterodimer collectively account for the selective impairment of the respiratory burst in some cell types in the patients carrying the Q231P or T178P allele.

#### **The mutant *CYBB* alleles are hypomorphic in CHO cells**

We additionally characterized the two *CYBB* mutant alleles Q231P and T178P in a gp91<sup>phox</sup>-deficient Chinese Hamster Ovary (CHO) epithelial cell line, in which gp91<sup>phox</sup> can be expressed at higher levels upon transfection, allowing a fine study of its biochemical processing and association with p22<sup>22-24,36-38</sup>. In CHO and other heterologous cells, as well as in EBV-B cells<sup>20,21,28</sup>, unassembled subunits are more stable than in granulocytes where these are rapidly degraded by the cytosolic proteasome<sup>23</sup>. The detection of the *CYBB*-encoded gp65 intermediate in macrophages and EBV-B cells from each kindred (**Fig. 5b, 5c**) suggested an underlying impairment in maturation to gp91<sup>phox</sup> that occurs after formation of the flavocytochrome b heterodimer. In CHO cells transduced with retroviral vectors for expression of either the wild-type, Q231P or T178P *CYBB* alleles, similar amounts of the gp65 form were detected (**Fig. 6a**

and **6b**). The co-expression of wild-type p22<sup>phox</sup> with wild-type CYBB increased cellular levels of mature 91 kDa gp91<sup>phox</sup> (**Fig. 6a** and **6b**). With co-expression of p22<sup>phox</sup>, mature T178P-gp91<sup>phox</sup> was produced in almost normal amounts in the cell and on its surface, whereas Q231P-gp91<sup>phox</sup> was produced in much smaller quantities; for both mutant alleles, substantial gp65 precursor was still present (**Fig. 6a** and **6b**). Thus, these findings suggest that there are no intrinsic problems in stability of the gp65 precursors encoded by two *CYBB* missense alleles but, rather, provide further evidence that the products of these alleles have reduced heterodimer formation with p22<sup>phox</sup> and subsequent maturation to the mature gp91<sup>phox</sup>, with the Q231P allele being more severely hypomorphic than the T178P allele, similar to the findings in patients' myeloid cells.

#### **The mutant *CYBB* alleles are hypomorphic in PLB-985 cells**

We then used an XR-CGD gp91<sup>phox</sup>-deficient myelomonocytic PLB-985 cell line<sup>35</sup>, which we also transduced with retroviral vectors for constitutive expression of wild-type-, Q231P- and T178P-gp91<sup>phox</sup>. In the undifferentiated myelomonocytic cells, gp91<sup>phox</sup> was detected in cells transduced with wild-type *CYBB*, whereas only small amounts of gp91<sup>phox</sup> were detected following transduction with either of the mutant *CYBB* alleles, although the gp65 precursor was present (**Fig. 6c**). The mature T178P-gp91<sup>phox</sup> was again produced in larger amounts than Q231P-gp91<sup>phox</sup>. When the cell line was induced to differentiate into granulocytes, the two mutant alleles remained hypomorphic, with reduced levels of gp91<sup>phox</sup> (**Fig. 6c**). As for fresh granulocytes from the patients, substantial respiratory burst activity relative to the amount of mature gp91<sup>phox</sup> was supported by the mutant alleles in the granulocyte-differentiated cells (not shown). By contrast, gp91<sup>phox</sup> was not expressed by the non transduced XR-CGD PLB-985 cell line, in which no respiratory burst was detectable. We also examined the levels of endogenous and of retrovirus-expressed gp91<sup>phox</sup> following differentiation into monocyte-like or macrophage-like cells with



either vitamin D<sup>39</sup> or a combination of vitamin D and PMA<sup>40</sup>, respectively. In wild-type PLB-985 cells, endogenous gp91<sup>phox</sup> expression increased with either of these regimens (**Fig. 6d**). The level of wild-type gp91<sup>phox</sup> expressed using the constitutively active retroviral vector was similar in undifferentiated cells and following either type of differentiation (**Fig. 6d**). In contrast, retrovirus-mediated expression of gp91<sup>phox</sup> harboring either the T178P or Q231P mutation was lower than that of wild-type gp91<sup>phox</sup>, and decreased even further following macrophage differentiation (**Fig. 6d**). These experiments demonstrate that the Q231P and T178P alleles are hypomorphic in the myelomonocytic PLB-985 cell line. Although expression of the gp65 precursor of gp91<sup>phox</sup> was relatively preserved with either of these two mutations, there was reduced, but not abolished expression, of gp91<sup>phox</sup> itself, consistent with impaired flavocytochrome-b<sub>558</sub> formation, particularly following macrophage differentiation.

## Discussion

We report here the first germline mutations in *CYBB* conferring the phenotype of XR-MSMD but not XR-CGD or “variant XR-CGD”. Six otherwise healthy and maternally-related male adults with BCG-disease and another with *bona fide* tuberculosis had XR-MSMD-2, due to inheritance of the Q231P or T178P *CYBB* allele. The two missense mutations are intrinsically and severely hypomorphic in gp91<sup>phox</sup>-deficient cells as diverse as EBV-B cells, CHO cells, and PLB-985 cells. *CYBB* is a novel Mendelian mycobacterial susceptibility gene, the seventh MSMD- and second XR-MSMD-causing gene identified, and the fifth tuberculosis-predisposing gene (after *IFNGR1*, *IL12B*, *IL12RB1*, and *NEMO*)<sup>2,3</sup>. It is the first shown to affect the respiratory burst. The physiological links between *CYBB* and the formerly identified MSMD-causing and tuberculosis-predisposing genes involved in the IL-12-IFN- $\gamma$  circuit remain to be unraveled. The cellular predisposing genes involved in the IL-12-IFN- $\gamma$  circuit remain to be unraveled. The cellular phenotype of this defect is uniform and different from that of CGD and “variant CGD”: the respiratory burst in MDMs or EBV-B cells from the seven patients tested was severely impaired, whereas their PMNs and monocytes showed no such dysfunction. The *CYBB* Q231P and T178P alleles are therefore severely hypomorphic in a cell-specific manner, providing an example of a human genetic illness resembling the phenotype of ‘conditional knockout’ mice, with the nuance that gene ablation in one of the two affected lineages also depends on cell differentiation (monocyte to macrophage). *CYBB* is a human gene for which alleles null in all cells (in particular all phagocytes, resulting in CGD) and now in selected cell types (in particular in macrophages, resulting in MSMD) have been identified and shown to produce different phenotypes. The mechanism underlying the B cell- and macrophage-specific effects of these germline mutations, which result in impaired but not absent flavocytochrome b<sub>558</sub> assembly, is related to cell-specific differences in gp91<sup>phox</sup> expression, in the threshold of gp91<sup>phox</sup> expression required for

flavocytochrome-b<sub>558</sub> complex assembly, and in the threshold of assembled b<sub>558</sub> complex required for NADPH oxidase activity. The clear-cut dichotomy between cells with an entirely normal (PMNs, monocytes) respiratory burst and those with a severely impaired (MDMs, EBV-B cells) respiratory burst was remarkable. Further studies are required to test the impact of these two mutations on the respiratory burst of dendritic cells<sup>41</sup>.

Our study suggests that the respiratory burst in human tissue macrophages is critical for immunity against tuberculous mycobacteria. It is already clear from human patients with CGD<sup>11</sup> that the respiratory burst plays an important role in immunity to BCG and *M. tuberculosis*. Intriguingly, these patients are not prone to infections with environmental, non-tuberculous mycobacteria, even species more virulent than BCG in other patients with MSMD, implying that the respiratory burst is redundant for the macrophage destruction of most non-tuberculous mycobacteria. The growth of BCG was enhanced in the patients' MDMs *in vitro*, further suggesting that there is a specific requirement for NADPH oxidase assembly to control tuberculous mycobacteria in human macrophages *in vivo*. Other pathways possibly disrupted by the impairment of the respiratory burst in macrophages, such as IL-12 production or antigen presentation, may also contribute to the pathogenesis of mycobacterial diseases. The role of the respiratory burst in anti-mycobacterial immunity *in vivo* and *in vitro* has not been firmly established in the mouse model, in which nitric oxide plays a much more important role<sup>42-45</sup>. Further genetic approaches<sup>46,47</sup> may reveal the means by which the human respiratory burst controls tuberculous mycobacteria, and the role played by nitric oxide production against tuberculous or non tuberculous mycobacteria<sup>45</sup>. Conversely, our seven adult patients with MSMD (including a patient with tuberculosis) are clinically healthy and had no history of other granulomatous or infectious diseases. This strongly suggests that both the granulomatous disease, and the bacterial and fungal infections affecting patients with CGD or "variant CGD" reflect

447 additional dysfunctions of granulocytes and/or monocytes, rather than macrophage defects alone

448 <sup>48,49</sup>.

449

450

451

452

453

454

455

456

457

458

459

460

461

462

463

464

465

466

467

468

469

470

471

472

473

474

475

476

477

478

479

480

481

482

483

484

485

486

487

488

## Acknowledgments

We warmly thank family members for their kind willingness to participate in this study. We thank J. Curnutte for EBV-B cells from CGD controls, D. Roos for mAb449, F. Morel for mAb7A2 and M. Quinn for mAb54.1. We thank all members of the two branches of the laboratory of Human Genetics of Infectious Diseases for discussions and Tony Leclerc, Yoann Rose, Mbia Kezadi, and Natalie Stull for technical assistance. Jacinta Bustamante was supported by INSERM, EU grant NEOTIM EEA05095KKA, and March of Dimes (RO5050KK). A. Condino-Neto was supported by *Fundação de Amparo a Pesquisa do Estado de São Paulo* and *Conselho Nacional de Desenvolvimento Científico e Tecnológico* (CNPq). This work was supported by *Fondation BNP-Paribas*, *Fondation Schlumberger*, *Institut Universitaire de France*, the ANR, The Rockefeller University Center for Clinical and Translational Science grant number 5UL1RR024143-03, The Rockefeller University, EU grants HOMITB HEALTH-F3-2008-200732 and NEOTIM EEA05095KKA, NIH grants DK54369 (P.E.N.) and HL045635 (M.C.D.), and the Riley Children's Foundation (M.C.D.). Jean-Laurent Casanova was an International Scholar of the Howard Hughes Medical Institute (2005-2008).

## Author contributions

J.B., L.A. and J.-L.C. designed the study and contributed intellectually to the experimental process. Most experimental studies were performed by J.B. under the supervision of J.-L.C. A.A.A., C.C.M., E.V. and M.C.D. did the experiments with retroviral transduction of gp91<sup>phox</sup> in EBV-B, CHO and PLB-985 cells, G.V. made the non retroviral *CYBB* vectors, infected macrophages with BCG, and made an intellectual contribution to various experiments, C.P. contributed to the recruitment of the patients and initiated the clinical investigation, L.B.G., C.P.,

L.J., and M.H. analyzed a number of controls, A.C. carried out qRT-PCR, L.B. did some bioinformatics analysis, J.-F.E. carried out the histological analysis of lymph nodes, B.W. performed the immunoperoxidase staining, A.V.G., C.B. and A.B. provided the data for linkage analysis, A.P., J.F. and S.D.-B. provided important experimental advice concerning cell culture, J.-M.B., S.B., O.L., and C.G. contributed to the recruitment and follow-up of the patients and CGD controls, S.A., P.N., A.C.N. and M.C.D. provided CGD controls and intellectual guidance for the development of various assays, and J.B. and J.-L.C. wrote the paper. All authors commented on and discussed the paper.

#### **Competing interests statement**

The authors declare that they have no competing financial interests.

#### **Figure legends**

##### **Figure 1. Q231P and T178 *CYBB* mutations in an X-linked recessive form of MSMD-**

**type 2. a,** Pedigrees of the families with XR-MSMD-2, including only individuals selected for the X-chromosome scan. Generations are designated by a Roman numeral (I, II, III, IV, and V). Patients with BCG disease (P2, P3, P4, P5, P6 and P7) are represented by black symbols and patients with tuberculosis (P1, H1) by gray symbols. The probands are indicated by an arrow. The fifteen heterozygous female subjects are indicated by black dots. The two founders who must have carried the *CYBB* mutation but did not display any mycobacterial phenotype are indicated by a vertical bar. Individuals whose genetic status could not be evaluated are indicated by the symbol “E?”. All other family members are wild-type for *CYBB* and are shown in white. **b,**

Automated sequencing profile showing the Q231P and T178P *CYBB* mutations in cDNA extracted from EBV-B cells from the patients (P) and comparison with the sequence obtained from a control (C+). The A→C mutation leads to the replacement at residue 231 of Gln (Q) by Pro (P) or the replacement at residue 178 of Thr (T) by Pro (P). The mutations were confirmed in genomic DNA and cDNA for seven patients. **c**, Schematic representation of the topology model of gp91<sup>phox</sup> regions corresponding to (EC) extracellular, (TM) transmembrane and (IC) intracellular regions. Q231P is situated in the third extracellular loop and T178P is situated in the transmembrane region.

**Figure 2. Evaluation of NADPH oxidase activity in PMNs and monocytes.** Superoxide generation was measured by assaying SOD-inhibitable cytochrome-*c* reduction in **a**, PMNs and monocytes, after adding PMA (40 ng/ml), for healthy controls (C+, n=5 for PMNs, and n=6 for monocytes), CGD patients (C–, n=1) and patients (P-Q231P, n=4 and P-T178P, n=1). Assay carried out with and without catalase. For the 10 conditions displayed on panel A (6 for PMNs, 4 for monocytes), the levels of superoxide production were compared between C+ and the Q231P patients by a nonparametric Wilcoxon exact test, and no significant differences at the 0.01 level (accounting for multiple testing) were observed. Hydrogen peroxide release was evaluated by fluorometric quantification with *N*-acetyl-3, 7 dihydroxyphenoxazine in **b**, PMNs and monocytes, after adding PMA, for healthy controls (C+, n=11 for PMNs, and n=12 for monocytes), CGD patients (C–), and patients (P). Results are the means of duplicate determinations. Histograms for the flow cytometric analysis of intracellular H<sub>2</sub>O<sub>2</sub> production, (DHR123 test) in **c**, PMNs and monocytes from C+), an X-linked CGD patient (C–) and the P-Q231P before (dotted lines) and after (solid lines) stimulation with PMA (400 ng/ml). **d**, PMNs from C+, C–, P-Q231P and H (female heterozygous for the Q231P allele) were treated with or without TNF-α, IL-1β and

cytochalasin b, and stimulated with fMLF (DHR123 assay). The results shown are representative of two independent experiments. **e**, Killing of *Staphylococcus aureus* by granulocytes from C+ (n=4), CGD patients (n=3), and patients from kindreds A and B (n=2).

**Figure 3. Evaluation of NADPH oxidase activity in MDMs.**

Release of hydrogen peroxide from MDMs (M-CSF + IL-4) from healthy controls (C+, n=4), an X-linked CGD patient (C-, n=1), patients (P-Q231P, n=1 and P-T178P, n=1) and heterozygous females (H, n=4). MDMs (M-CSF + IL-4) were activated by incubation with (left panel) live BCG (10:1), (right panel) PPD (1 mg/ml), or (lower panel) IFN- $\gamma$  ( $10^5$  IU/ml) for 18 h and H<sub>2</sub>O<sub>2</sub> release was triggered with PMA (400 ng/ml). The results shown are representative of two independent experiments.

**Figure 4. Evaluation of NADPH oxidase activity in EBV-B cells.**

**a**, Superoxide production was measured by cytochrome-c reduction.  $10^6$  EBV-B cells from healthy controls (C+, n=22), an X-linked CGD patient (C-, n=4) and patients (P-Q231P, n=4 and P-T178P, n=3) were activated by incubation with 400 ng/ml PMA for 2 hours. Data are representative of two independent experiments. **b**, Hydrogen peroxide release by EBV-B cells from a healthy control (C+), seven patients (P1, P2, P3, P4, P5, P6 and P7), and an X-linked CGD patient (C-). EBV-B cells were activated with three doses of PMA, at four time points, expressed in minutes. **c**, NBT reduction by EBV-B cells after PMA activation (400 ng/ml). NBT-positive cells from a healthy control (C+), patients (P1, P2, P3, P4, P5, and P6) and an X-linked CGD patient (C-). **d**, Functional reconstitution of NADPH oxidase function in EBV-B cells using retroviral transduction. Cells from a XR-CGD patient were transduced with pMSCVPuro-gp91<sup>phox</sup>WT,



pMSCVPuro-gp91<sup>phox</sup>T178P and pMSCVPuro-gp91<sup>phox</sup>Q231P retroviral particles. Additionally, EBV-B cells obtained from T178P patients and healthy control (C+) were transduced with pMSCVPuro-gp91<sup>phox</sup>WT retroviral particles. Hydrogen peroxide release was assessed after 2 hours of PMA activation (400 ng/ml). The results shown are representative of two independent experiments.

**Figure 5. Expression of gp91<sup>phox</sup> and flavocytochrome-b<sub>558</sub> in the patients' cells.**

**a**, Immunoblot analysis using PMNs and monocytes from a healthy control (C+), gp91<sup>phox0</sup> (C-) and the patients (P-Q231P and P-T178P). Gp91<sup>phox</sup> protein was detected with three antibodies directed against gp91<sup>phox</sup>, 53 BD, 54.1, and 7A2; an antibody against GAPDH was used as a protein loading control. The results shown are representative of two independent experiments. **b**, Immunoblot analyses of PMNs, monocytes, MDMs (only M-CSF or M-CSF + IL-4) from a healthy C+, gp91<sup>phox0</sup> (C-) patient and patients (P-Q231P and P-T178P) using an antibody directed against gp91<sup>phox</sup> (mAb 54.1); an antibody against STAT1 was used as a protein loading control. **c**, EBV-B cell lysates were evaluated for gp91<sup>phox</sup> (mAb 54.1), p22<sup>phox</sup> and  $\beta$ -actin protein expression was used as a protein loading control (n=3). Left panel shows cell lysates of EBV-B cells from C+, XR-CGD, patient with deletion of *CYBB*, and the patients. The middle panel shows cell lysates of the same XR-CGD EBV-B cells transduced with pMSCVPuro-gp91<sup>phox</sup>WT, pMSCVPuro-gp91<sup>phox</sup>T178P and pMSCVPuro-gp91<sup>phox</sup>Q231P retroviral particles. The right panel shows cell lysates of EBV-B cells from C+ and XR-CGD, and patients and the same cells, except XR-CGD, transduced with pMSCVPuro-gp91<sup>phox</sup>WT. **d**, PMNs and monocytes and **e**, EBV-B cells from C+, a gp91<sup>phox0</sup> and the patients. Cell surface staining with

mAb7D5, (an antibody specific for gp91<sup>phox</sup>; solid lines); an isotype IgG1 (dotted lines). The results shown are representative of two independent experiments.

**Figure 6. Expression and function of mutant gp91<sup>phox</sup> in cell lines.** **a**, CHO and CHO22 cells were transduced with pMSCVPuro-gp91<sup>phox</sup>WT, pMSCVPuro-gp91<sup>phox</sup>T178P and pMSCVPuro-gp91<sup>phox</sup>Q231P retroviral particles, and then selected with puromycin. Cell lysates of the transduced cells, CHO, CHO22 and CHO<sup>phox</sup> cells were evaluated for gp91<sup>phox</sup> (mAb 54.1), p22<sup>phox</sup> (mAb NS5) to detect the gp91<sup>phox</sup> maturation and p22<sup>phox</sup> expression. An antibody against  $\beta$ -actin was used as a protein loading control. **b**, Cell surface gp91<sup>phox</sup> detected with 7D5 antibody using flow cytometry in CHO22 and CHO22 expressing gp91<sup>phox</sup> WT, gp91<sup>phox</sup> Q231P and gp91<sup>phox</sup> T178P. **c**, and **d**, PLB X-CGD cells were transduced with pMSCVPuro-gp91<sup>phox</sup>WT, pMSCVPuro-gp91<sup>phox</sup>T178P or pMSCVPuro-gp91<sup>phox</sup>Q231P retroviral particles, and then selected with puromycin. **c**, Lysates (20  $\mu$ g per well) prepared from PLB X-CGD transduced cells or PLB985 WT (1, 2.5 and 5  $\mu$ g per well) were evaluated for gp91<sup>phox</sup> (mAb 54.1) expression, as assessed in undifferentiated cells (–) or following day 6 of granulocyte differentiation induced with DMF (+). An antibody against  $\beta$ -actin was used as a protein loading control, and an antibody against p67<sup>phox</sup> was used to verify differentiation. **d**, Cells differentiated into monocyte-like cells or into macrophage-like cells. Cell lysates (20  $\mu$ g per well) were evaluated for gp91<sup>phox</sup> (mAb 54.1), and an antibody against p67<sup>phox</sup> was used to verify differentiation. Human polymorphonuclear neutrophils (PMNs) cell lysis (2.5  $\mu$ g) was also used as a control. The results shown are representative of three independent experiments.

## Methods

### Patients

In kindred A, four male subjects presented a selective predisposition to mycobacterial disease<sup>4</sup>. Briefly, patient 1 (P1) suffered from *bona fide* tuberculosis and three other patients (P2, P3 and P4) developed infection by *Mycobacterium bovis* BCG vaccine. They suffered from no other severe infections. These four patients remain otherwise healthy. A maternal aunt (H1) suffered from salpingitis and pulmonary tuberculosis.

All the members of kindred B are French and live in France. Three patients (P5, P6, and P7) suffered from BCG infection (see **Supplementary information**). No other unusual infections were reported in any of these three patients. Informed consent was obtained from all family members and our study was approved by the Necker and Rockefeller IRBs.

### DNA techniques, PCR and sequencing

Genomic DNA was extracted with phenol/chloroform. The sequences of the primers used for PCR amplification of *CYBB* exons and cDNA are available upon request.

### Preparation of PMNs, monocytes and MDMs

PMNs and monocytes were prepared from heparin-treated blood. Peripheral blood was subjected to dextran sedimentation and the buffy coat was centrifuged through Ficoll-Hypaque. The remaining red blood cells were removed by hypotonic shock.

Monocytes were isolated by positive immunomagnetic depletion (CD14 MicroBeads, Miltenyi Biotec). MDMs were obtained from purified monocytes cultured in the presence of M-CSF (50 ng/ml; R&D Systems). We plated  $2 \times 10^4$  monocytes or MDMs per well in complete RPMI 1640 medium (RPMI medium supplemented with 10% heat-inactivated pooled FBS

(GIBCO BRL)) in 96-well plates (Nunc) and incubated them at 37°C in an atmosphere containing 5% CO<sub>2</sub>. One type of MDMs differentiated with M-CSF were obtained by adding, on day 7, *Salmonella minnesota* LPS (Sigma-Aldrich, 1 µg/ml) + IFN-γ (10<sup>5</sup> IU/ml, Imukin, Boehringer Ingelheim). The incubation was continued until day 16 to 17. Finally, other MDMs differentiated with M-CSF were obtained by adding IL-4 (50 ng/ml; R&D Systems) on day 7 and incubating until day 16 to 17<sup>16</sup>.

### **Superoxide assay**

PMNs and monocytes were stimulated with 40 ng/ml of 4-beta-phorbol 12-beta-myristate 13-alpha-acetate (PMA, Sigma Aldrich) in the presence or absence of 140 IU/ml catalase (Sigma Aldrich). EBV-B cells were stimulated for 2 hours at 37°C. Superoxide release was assessed by the SOD-inhibitable cytochrome-*c* reduction assay, as previously reported<sup>19</sup>.

### **Hydrogen peroxide assay**

Cells were stimulated with PMA at 37°C. EBV-B cells and measured hydrogen peroxide according to the kit manufacturer's (Amplex Red reagent: 10-acetyl-3,7-dihydroxyphenoxazine; Molecular Probes, Invitrogen). The hydrogen peroxide released was quantified with Victor<sup>TM</sup>X4 (Perkin Elmer). MDMs were cultured for 16 to 18 hours with live BCG (*Mycobacterium bovis* BCG, Pasteur substrain at a multiplicity of infection of 10:1), PPD (1 mg/ml, Tuberculin PPD Batch RT49, Statens Serum Institute, Denmark) or IFN-γ (10<sup>5</sup> IU/ml; Imukin, Boehringer Ingelheim), then washed in KRPS and activated by incubation for 30 min with PMA (400 ng/ml) or left unactivated.

**DHR assay**

Peripheral leukocytes were incubated with dihydrorhodamine 123 (DHR; Sigma Aldrich) at 37°C for 5 minutes in the presence of catalase (1,300 IU/ml; Sigma Aldrich), and after activation with PMA for 30 minutes. The leukocytes were first treated with TNF- $\alpha$  (20 ng/ml; R&D Systems), IL-1 $\beta$  (40 ng/ml; R&D Systems) or cytochalasin b (10  $\mu$ g/ml; Sigma-Aldrich) for 10 minutes at 37°C and were then stimulated with fMLF (80  $\mu$ g/ml; Sigma Aldrich) for 20 minutes. 10,000 or 5,000 events were recorded by flow cytometry on a FACScan or FACS Canto II machine (Becton Dickinson).

**NBT reduction**

Coverslips (10 mm) were placed in 24-well plates (Nunc), and  $2 \times 10^5$  MDMs per well were plated in complete RPMI 1640 medium and incubated at 37°C under an atmosphere containing 5% CO<sub>2</sub> for 16 to 17 days. After 18 hours of incubation with live BCG (10:1) or PPD (1 mg/ml), the MDMs were or were not exposed to PMA (400 ng/ml), in the presence of NBT (200  $\mu$ g/ml, Sigma Aldrich) in HBSS at 37°C for 1 hour, and were then counterstained by incubation with safranin (1%) for 10 minutes. The percentage of NBT-positive cells (blue formazan dye) was determined by light microscopy (QCapture), scoring 100 cells. EBV-B cells were activated by incubation with PMA for 2 hours at 37°C.

**Immunoblotting**

Cell lysates were analyzed by immunoblotting as described<sup>37</sup>. The membrane was incubated overnight with antibodies against gp91<sup>phox</sup> (BD Biosciences- clone 53,54.1 and 7A2 ).

For p22<sup>phox</sup> (SC-20781), p47<sup>phox</sup> (SC-14015), p67<sup>phox</sup> (SC-7663), and GAPDH (SC-25778), we used polyclonal antibodies from Santa Cruz.

#### **Flow cytometric detection of flavocytochrome-b<sub>558</sub>**

Cells were incubated with 7D5 antibody (MBL Co., Ltd., Japan) or isotypic control (mouse IgG1, BD PharMingen) at a concentration of 5 µg/ml, and at 4°C for 30 minutes. Cells were analyzed with a FACScan flow cytometer or FACS Canto II (Becton Dickinson). 10,000 or 5,000 cells from each sample were collected and analyzed with Cell Quest software (BD Pharmingen).

#### **Microbicidal assay with *Staphylococcus aureus***

Granulocytes were diluted in RPMI and *Staphylococcus aureus* (Calbiochem) in RPMI supplemented with 10 % pooled human serum. After preopsonisation of the bacteria, 2 x 10<sup>6</sup> granulocytes/ml were mixed with 2 x 10<sup>7</sup>/ml *S. aureus* CFU/ml, in a 14 ml round-bottomed polypropylene tube (Falcon). The tubes were incubated, at 37°C for 30 minutes at 100 x g. The cell suspensions were then centrifuged at 160 x g and 4°C for 10 minutes. The supernatant was removed and the cell pellets were resuspended in 1 ml of RPMI with 100 µg/ml of gentamicin and incubated at 37°C for 4 times at 100 x g. The samples were centrifuged at 160 x g at 4°C for 10 minutes. The granulocytes were lysed with 200 µl of 0.1% Triton. CFU bacteria was counted by plating serial dilutions after incubation.

#### **Retroviral transduction of EBV-B, CHO, and PLB-985 cells**

A human cDNAs encoding the gp91<sup>phox</sup> WT, gp91<sup>phox</sup>T178P and gp91<sup>phox</sup>Q231P were cloned into pMSCVpuro (Clontech). Retroviral vectors were packaged using the Pantropic

Retroviral Expression System (BD Clontech). EBV-B cells, CHO22 cells generated for stable expression of untagged p22<sup>phox</sup> and promyelocytic PLB-985 harboring a disrupted *CYBB* (PLB X-CGD cells) were transduced with MSCVPuro-gp91<sup>phox</sup>WT, MSCVPuro-gp91<sup>phox</sup>Q231P or MSCVPuro-gp91<sup>phox</sup>T178P retrovirus. CHO-K1 cell lines utilized in these studies were generated previously<sup>36,38</sup>. For neutrophil and monocyte-macrophage differentiations, PLB-985 or PLB XR-CGD cells were cultured as previously described<sup>35,50</sup>.

## References

1. Casanova, J.L. & Abel, L. Genetic dissection of immunity to mycobacteria: the human model. *Annu Rev Immunol* **20**, 581-620 (2002).
2. Alcais, A., Fieschi, C., Abel, L. & Casanova, J.L. Tuberculosis in children and adults: two distinct genetic diseases. *J Exp Med* **202**, 1617-21 (2005).
3. Filipe-Santos, O. et al. Inborn errors of IL-12/23- and IFN-gamma-mediated immunity: molecular, cellular, and clinical features. *Semin Immunol* **18**, 347-61 (2006).
4. Bustamante, J. et al. A novel X-linked recessive form of Mendelian susceptibility to mycobacterial disease. *J Med Genet* **44**, e65 (2007).
5. Filipe-Santos, O. et al. X-linked susceptibility to mycobacteria is caused by mutations in NEMO impairing CD40-dependent IL-12 production. *J Exp Med* **203**, 1745-59 (2006).
6. Notarangelo, L.D. et al. Primary immunodeficiencies: 2009 update. *J Allergy Clin Immunol* **124**, 1161-78 (2009).
7. Roos, D. et al. Hematologically important mutations: X-linked chronic granulomatous disease (third update). *Blood Cells Mol Dis* **45**, 246-65 (2010).
8. Mouy, R., Fischer, A., Vilmer, E., Seger, R. & Griscelli, C. Incidence, severity, and prevention of infections in chronic granulomatous disease. *J Pediatr* **114**, 555-60 (1989).
9. Segal, B.H., Leto, T.L., Gallin, J.I., Malech, H.L. & Holland, S.M. Genetic, biochemical, and clinical features of chronic granulomatous disease. *Medicine (Baltimore)* **79**, 170-200 (2000).
10. Winkelstein, J.A. et al. Chronic granulomatous disease. Report on a national registry of 368 patients. *Medicine (Baltimore)* **79**, 155-69 (2000).
11. Bustamante, J. et al. BCG-osis and tuberculosis in a child with chronic granulomatous disease. *J Allergy Clin Immunol* **120**, 32-8 (2007).
12. Lee, P.P. et al. Susceptibility to mycobacterial infections in children with X-linked chronic granulomatous disease: a review of 17 patients living in a region endemic for tuberculosis. *Pediatr Infect Dis J* **27**, 224-30 (2008).
13. van den Berg, J.M. et al. Chronic granulomatous disease: the European experience. *PLoS One* **4**, e5234 (2009).
14. Mohanty, J.G., Jaffe, J.S., Schulman, E.S. & Raible, D.G. A highly sensitive fluorescent micro-assay of H<sub>2</sub>O<sub>2</sub> release from activated human leukocytes using a dihydroxyphenoxazine derivative. *J Immunol Methods* **202**, 133-41 (1997).
15. Nakagawara, A., Nathan, C.F. & Cohn, Z.A. Hydrogen peroxide metabolism in human monocytes during differentiation in vitro. *J Clin Invest* **68**, 1243-52 (1981).
16. Martinez, F.O., Gordon, S., Locati, M. & Mantovani, A. Transcriptional profiling of the human monocyte-to-macrophage differentiation and polarization: new molecules and patterns of gene expression. *J Immunol* **177**, 7303-11 (2006).
17. Reichenbach, J. et al. Mycobacterial diseases in primary immunodeficiencies. *Curr Opin Allergy Clin Immunol* **1**, 503-11 (2001).
18. Conley, M.E. et al. Primary B cell immunodeficiencies: comparisons and contrasts. *Annu Rev Immunol* **27**, 199-227 (2009).
19. Condino-Neto, A. & Newburger, P.E. NADPH oxidase activity and cytochrome b558 content of human Epstein-Barr-virus-transformed B lymphocytes correlate with expression of genes encoding components of the oxidase system. *Arch Biochem Biophys* **360**, 158-64 (1998).

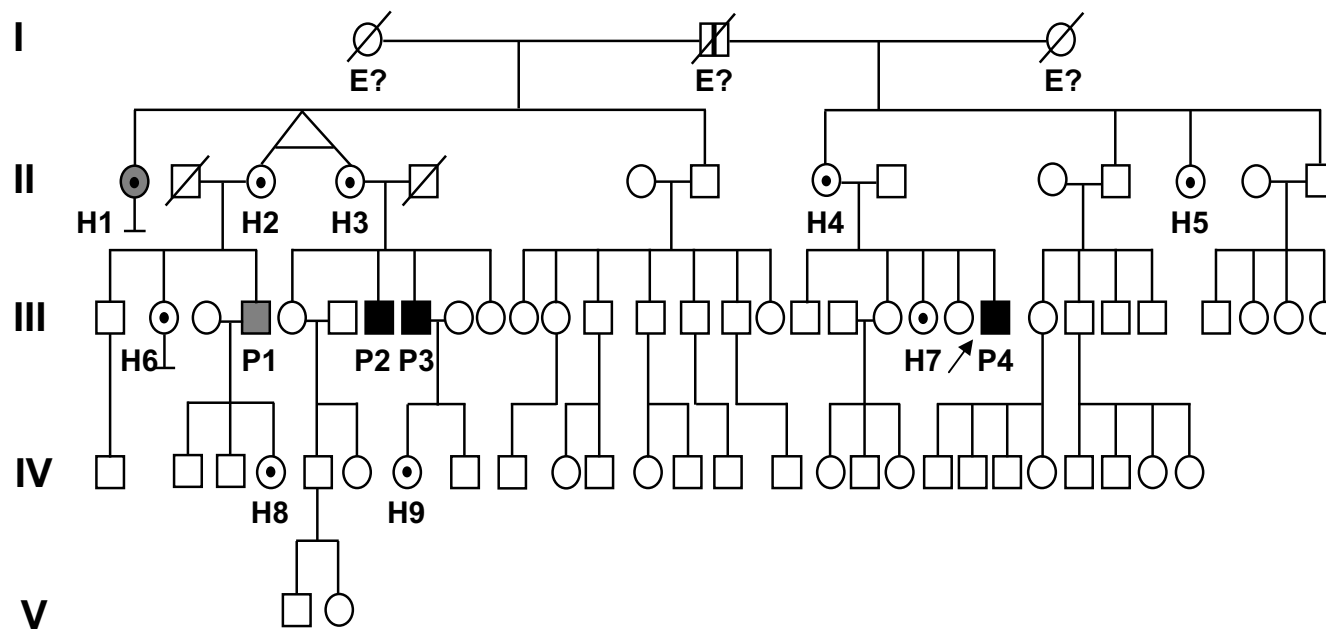


20. Porter, C.D. et al. p22-phox-deficient chronic granulomatous disease: reconstitution by retrovirus-mediated expression and identification of a biosynthetic intermediate of gp91-phox. *Blood* **84**, 2767-75 (1994).
21. Maly, F.E. et al. Restitution of superoxide generation in autosomal cytochrome-negative chronic granulomatous disease (A22(0) CGD)-derived B lymphocyte cell lines by transfection with p22phox cDNA. *J Exp Med* **178**, 2047-53 (1993).
22. Yu, L. et al. Biosynthesis of flavocytochrome b558 . gp91(phox) is synthesized as a 65-kDa precursor (p65) in the endoplasmic reticulum. *J Biol Chem* **274**, 4364-9 (1999).
23. DeLeo, F.R. et al. Processing and maturation of flavocytochrome b558 include incorporation of heme as a prerequisite for heterodimer assembly. *J Biol Chem* **275**, 13986-93 (2000).
24. Yu, L., Zhen, L. & Dinauer, M.C. Biosynthesis of the phagocyte NADPH oxidase cytochrome b558. Role of heme incorporation and heterodimer formation in maturation and stability of gp91phox and p22phox subunits. *J Biol Chem* **272**, 27288-94 (1997).
25. Nakamura, M., Murakami, M., Koga, T., Tanaka, Y. & Minakami, S. Monoclonal antibody 7D5 raised to cytochrome b558 of human neutrophils: immunocytochemical detection of the antigen in peripheral phagocytes of normal subjects, patients with chronic granulomatous disease, and their carrier mothers. *Blood* **69**, 1404-8 (1987).
26. Biberstine-Kinkade, K.J. et al. Heme-ligating histidines in flavocytochrome b(558): identification of specific histidines in gp91(phox). *J Biol Chem* **276**, 31105-12 (2001).
27. Heyworth, P.G. et al. Hematologically important mutations: X-linked chronic granulomatous disease (second update). *Blood Cells Mol Dis* **27**, 16-26 (2001).
28. Porter, C.D., Kuribayashi, F., Parkar, M.H., Roos, D. & Kinnon, C. Detection of gp91-phox precursor protein in B-cell lines from patients with X-linked chronic granulomatous disease as an indicator for mutations impairing cytochrome b558 biosynthesis. *Biochem J* **315 ( Pt 2)**, 571-5 (1996).
29. Yamauchi, A. et al. Location of the epitope for 7D5, a monoclonal antibody raised against human flavocytochrome b558, to the extracellular peptide portion of primate gp91phox. *Microbiol Immunol* **45**, 249-57 (2001).
30. Burritt, J.B. et al. Phage display epitope mapping of human neutrophil flavocytochrome b558. Identification of two juxtaposed extracellular domains. *J Biol Chem* **276**, 2053-61 (2001).
31. Cassatella, M.A. et al. Molecular basis of interferon-gamma and lipopolysaccharide enhancement of phagocyte respiratory burst capability. Studies on the gene expression of several NADPH oxidase components. *J Biol Chem* **265**, 20241-6 (1990).
32. Ezekowitz, R.A., Dinauer, M.C., Jaffe, H.S., Orkin, S.H. & Newburger, P.E. Partial correction of the phagocyte defect in patients with X-linked chronic granulomatous disease by subcutaneous interferon gamma. *N Engl J Med* **319**, 146-51 (1988).
33. Ding, C. et al. High-level reconstitution of respiratory burst activity in a human X-linked chronic granulomatous disease (X-CGD) cell line and correction of murine X-CGD bone marrow cells by retroviral-mediated gene transfer of human gp91phox. *Blood* **88**, 1834-40 (1996).
34. Ezekowitz, R.A. et al. Restoration of phagocyte function by interferon-gamma in X-linked chronic granulomatous disease occurs at the level of a progenitor cell. *Blood* **76**, 2443-8 (1990).

35. Zhen, L. et al. Gene targeting of X chromosome-linked chronic granulomatous disease locus in a human myeloid leukemia cell line and rescue by expression of recombinant gp91phox. *Proc Natl Acad Sci U S A* **90**, 9832-6 (1993).
36. Casbon, A.J., Allen, L.A., Dunn, K.W. & Dinanuer, M.C. Macrophage NADPH oxidase flavocytochrome B localizes to the plasma membrane and Rab11-positive recycling endosomes. *J Immunol* **182**, 2325-39 (2009).
37. Zhu, Y. et al. Deletion mutagenesis of p22phox subunit of flavocytochrome b558: identification of regions critical for gp91phox maturation and NADPH oxidase activity. *J Biol Chem* **281**, 30336-46 (2006).
38. Biberstine-Kinkade, K.J. et al. Mutagenesis of p22(phox) histidine 94. A histidine in this position is not required for flavocytochrome b558 function. *J Biol Chem* **277**, 30368-74 (2002).
39. Perkins, S.L., Link, D.C., Kling, S., Ley, T.J. & Teitelbaum, S.L. 1,25-Dihydroxyvitamin D3 induces monocytic differentiation of the PLB-985 leukemic line and promotes c-fgr mRNA expression. *J Leukoc Biol* **50**, 427-33 (1991).
40. Jitkaew, S., Witasp, E., Zhang, S., Kagan, V.E. & Fadeel, B. Induction of caspase- and reactive oxygen species-independent phosphatidylserine externalization in primary human neutrophils: role in macrophage recognition and engulfment. *J Leukoc Biol* **85**, 427-37 (2009).
41. Savina, A. et al. NOX2 controls phagosomal pH to regulate antigen processing during crosspresentation by dendritic cells. *Cell* **126**, 205-18 (2006).
42. Adams, L.B., Dinanuer, M.C., Morgenstern, D.E. & Krahenbuhl, J.L. Comparison of the roles of reactive oxygen and nitrogen intermediates in the host response to Mycobacterium tuberculosis using transgenic mice. *Tuber Lung Dis* **78**, 237-46 (1997).
43. Segal, B.H. et al. The p47(phox/-) mouse model of chronic granulomatous disease has normal granuloma formation and cytokine responses to Mycobacterium avium and Schistosoma mansoni eggs. *Infect Immun* **67**, 1659-65 (1999).
44. Nathan, C. & Shiloh, M.U. Reactive oxygen and nitrogen intermediates in the relationship between mammalian hosts and microbial pathogens. *Proc Natl Acad Sci U S A* **97**, 8841-8 (2000).
45. MacMicking, J., Xie, Q.W. & Nathan, C. Nitric oxide and macrophage function. *Annu Rev Immunol* **15**, 323-50 (1997).
46. Casanova, J.L. & Abel, L. Primary immunodeficiencies: a field in its infancy. *Science* **317**, 617-9 (2007).
47. Alcais, A., Abel, L. & Casanova, J.L. Human genetics of infectious diseases: between proof of principle and paradigm. *J Clin Invest* **119**, 2506-14 (2009).
48. Gordon, S. & Taylor, P.R. Monocyte and macrophage heterogeneity. *Nat Rev Immunol* **5**, 953-64 (2005).
49. Segal, A.W. How neutrophils kill microbes. *Annu Rev Immunol* **23**, 197-223 (2005).
50. Price, M.O. et al. Creation of a genetic system for analysis of the phagocyte respiratory burst: high-level reconstitution of the NADPH oxidase in a nonhematopoietic system. *Blood* **99**, 2653-61 (2002).

a

## Kindred A



## Kindred B

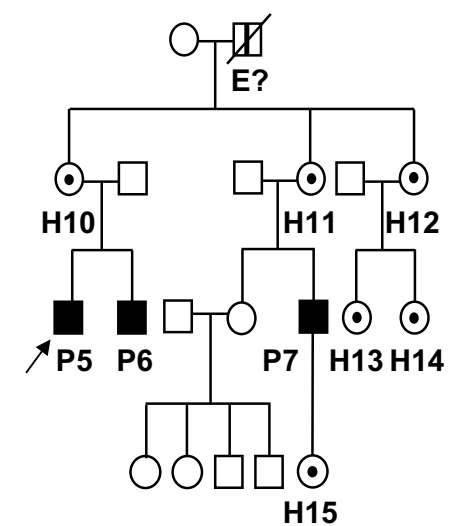
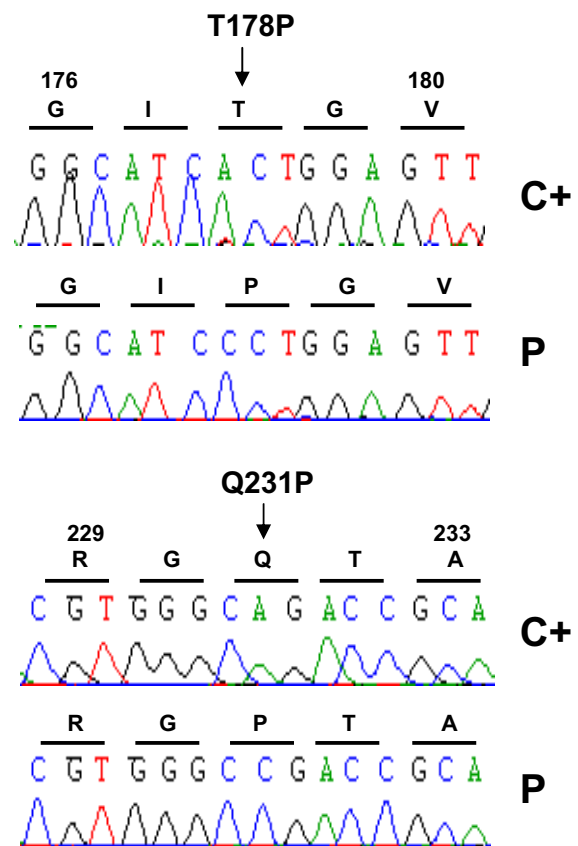


Figure 1

b



c

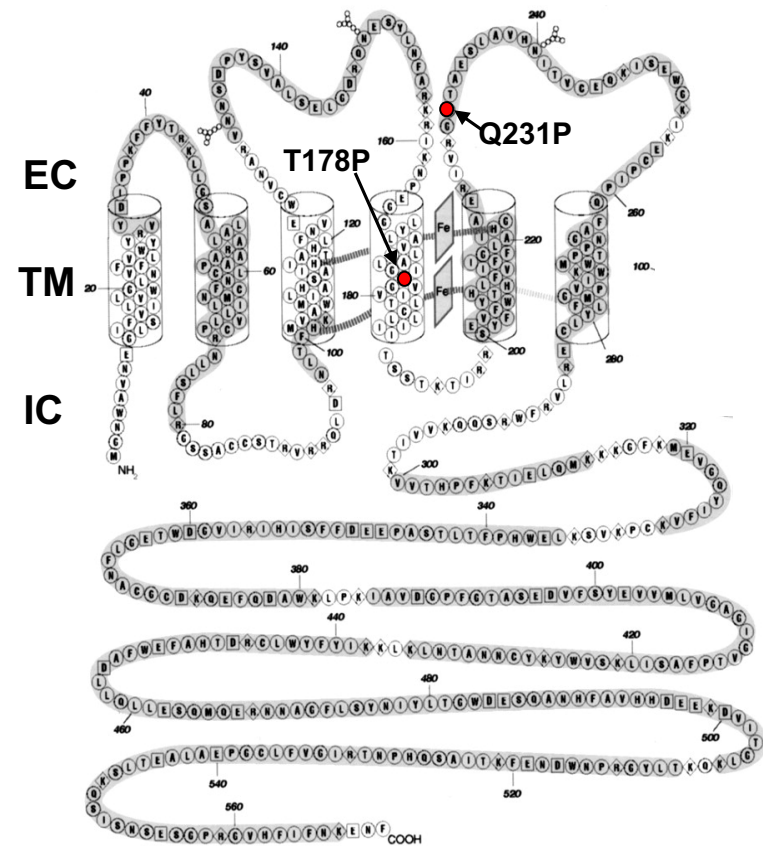
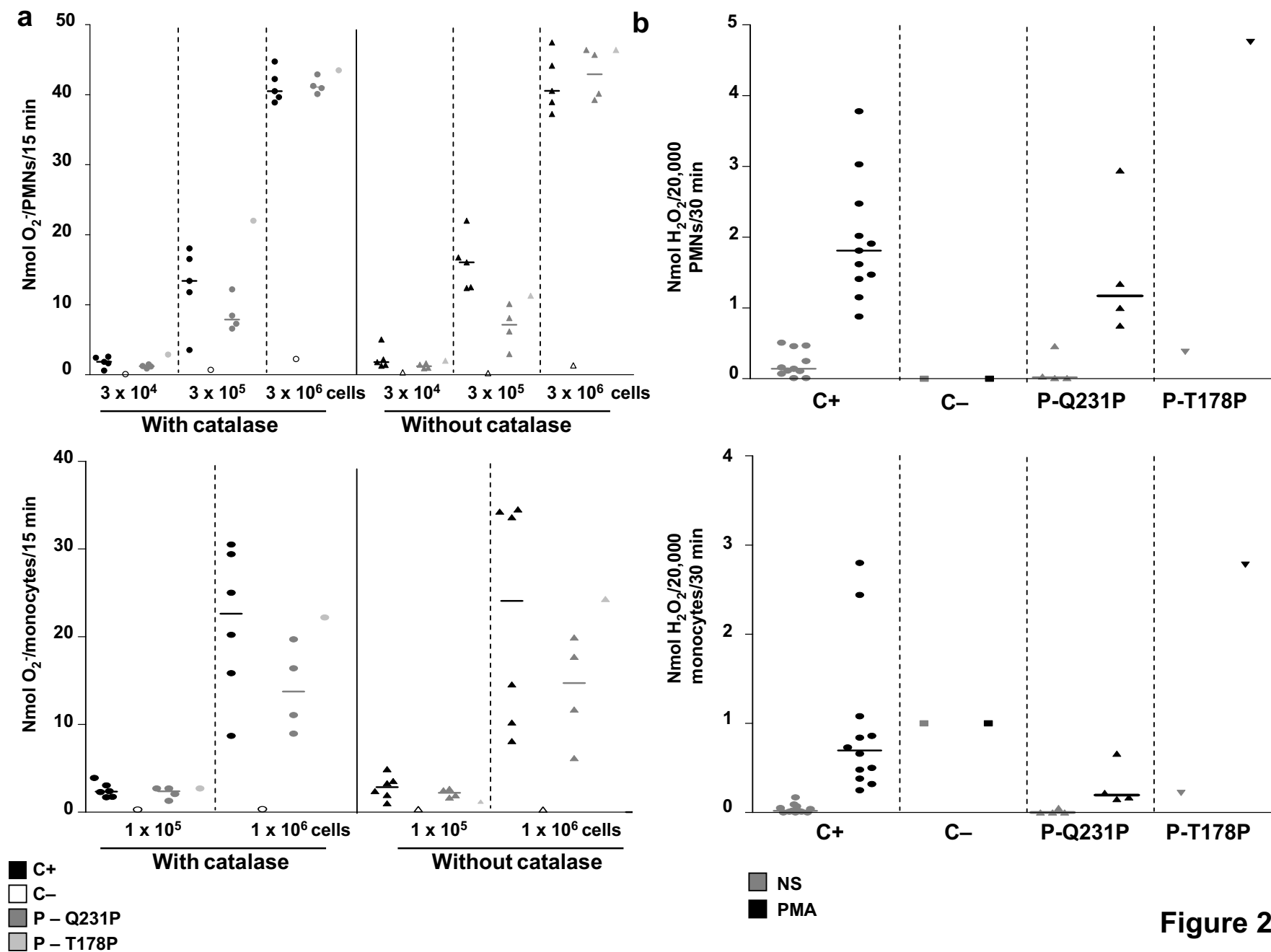
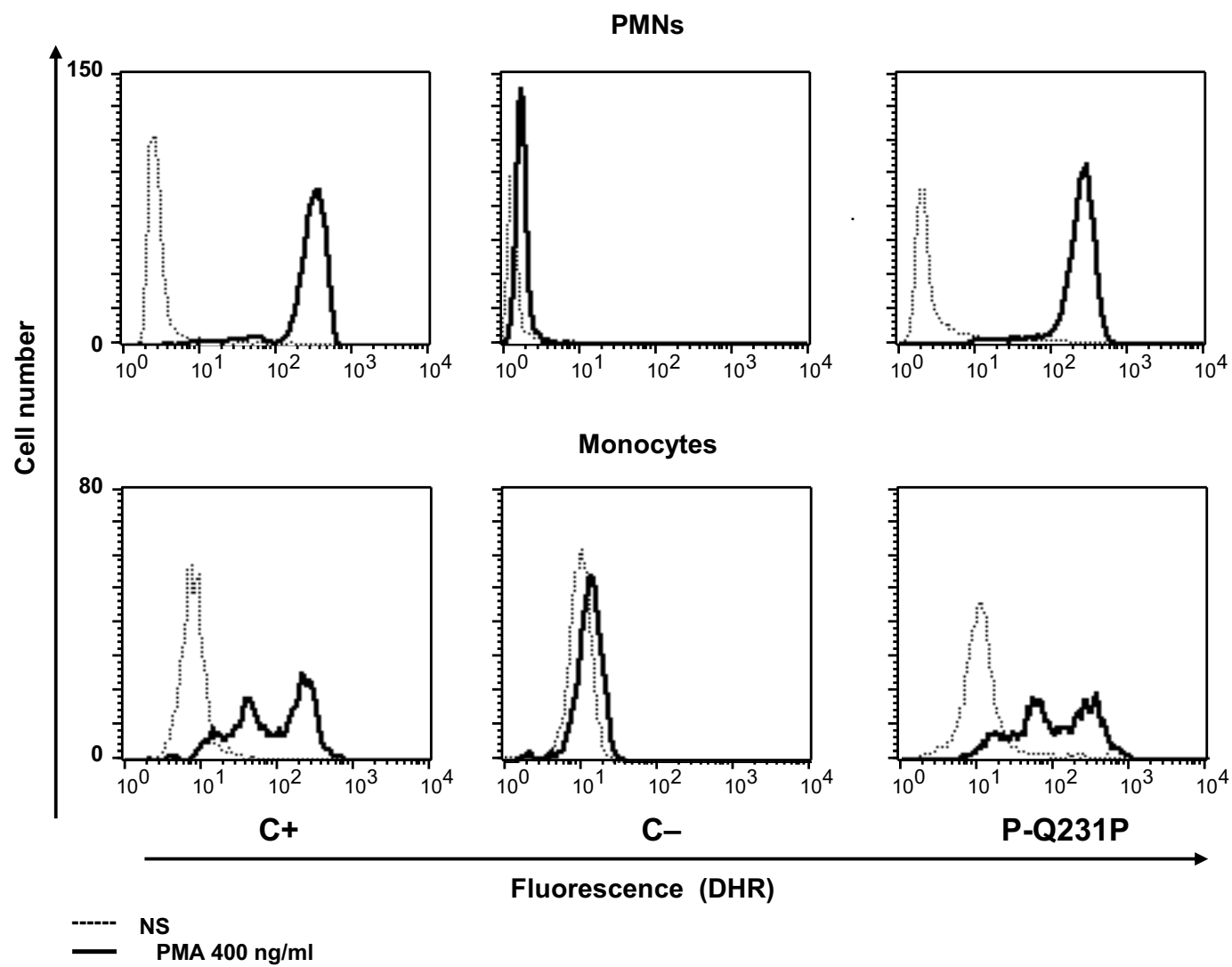


Figure 1



**Figure 2**

**C****Figure 2**

d

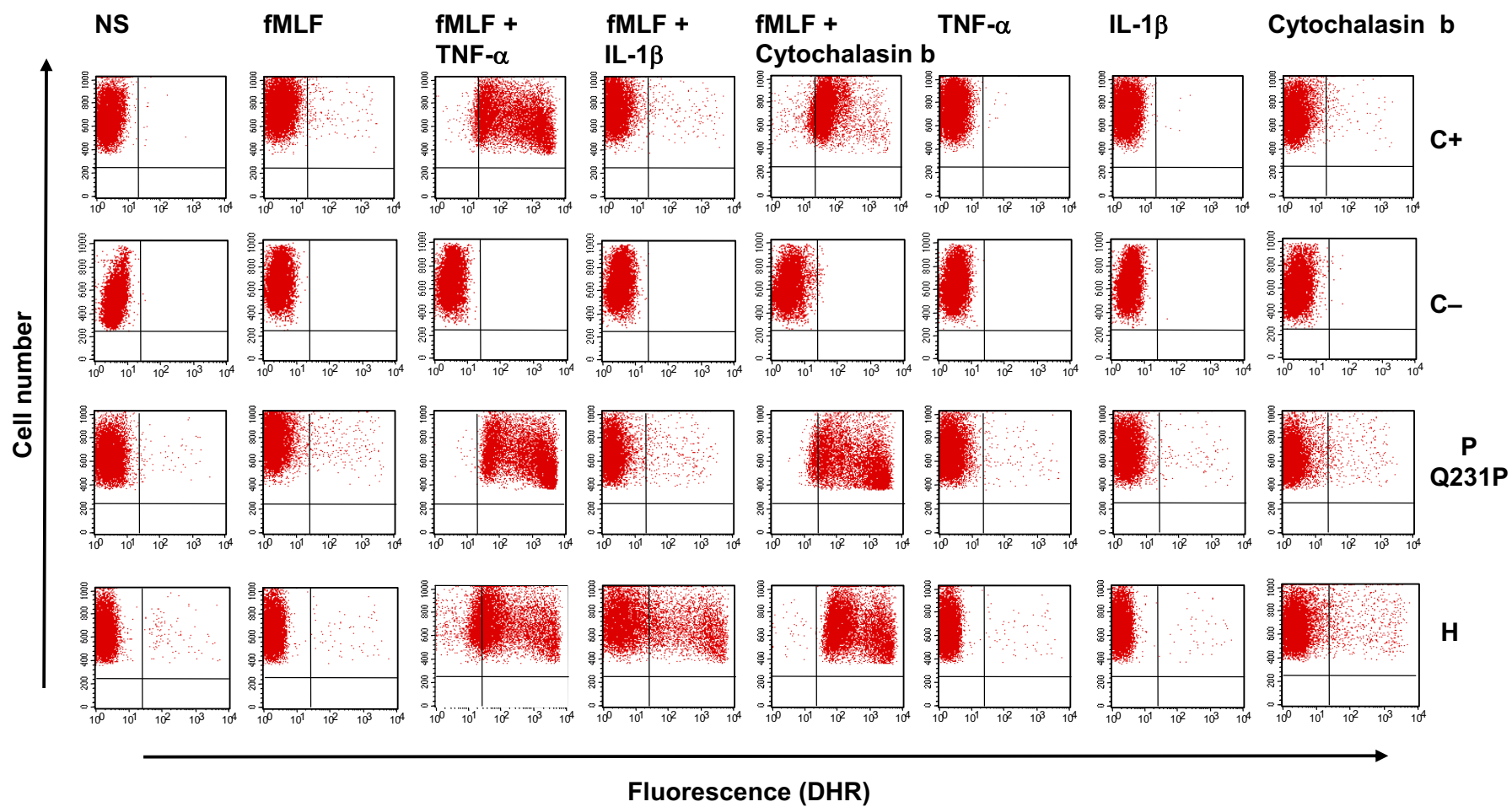


Figure 2

e

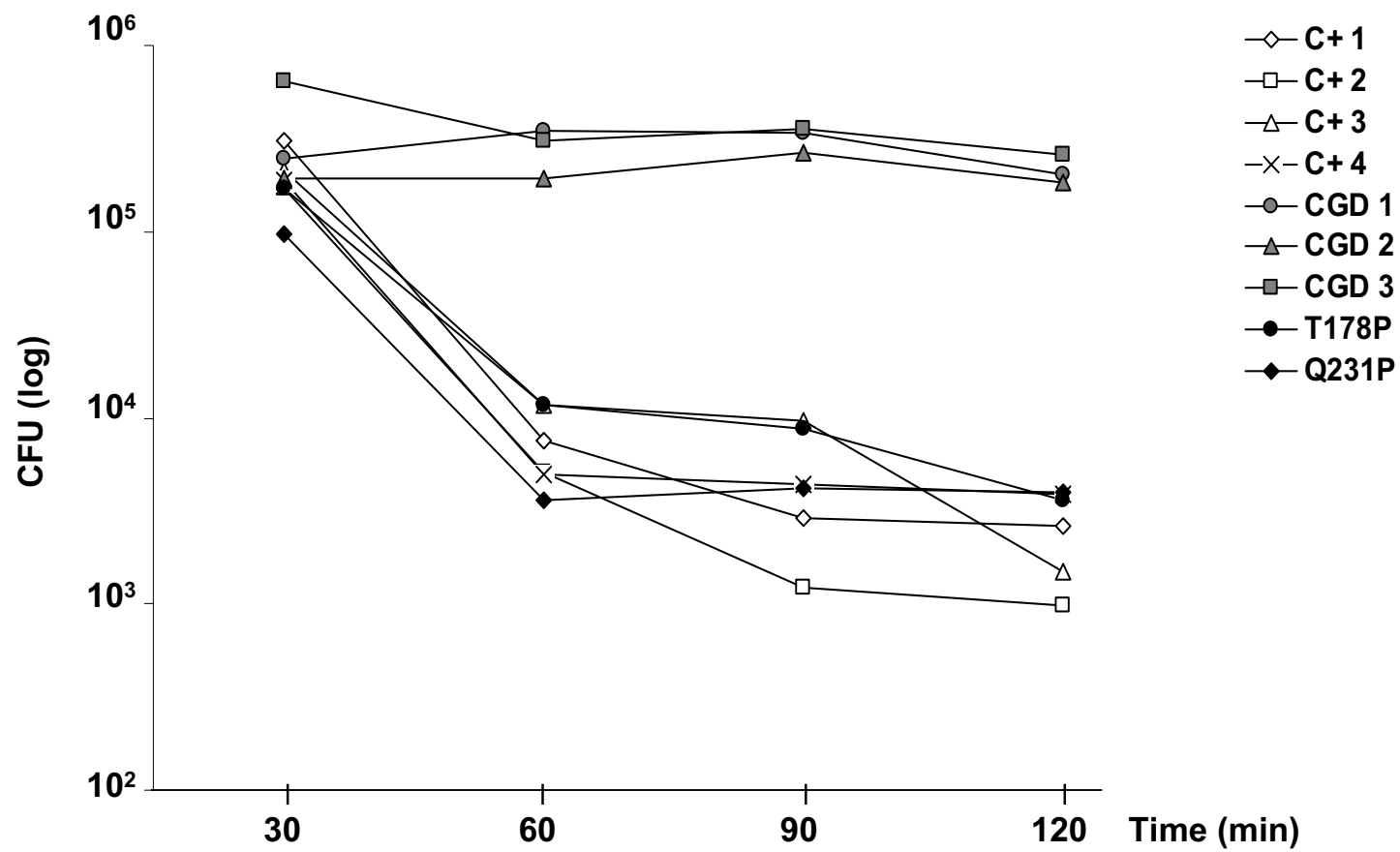


Figure 2



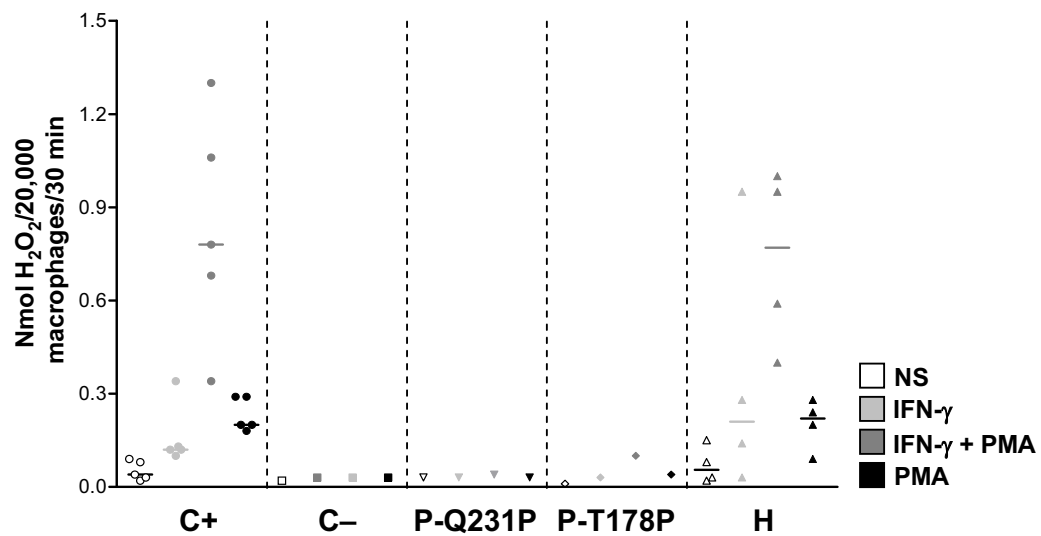
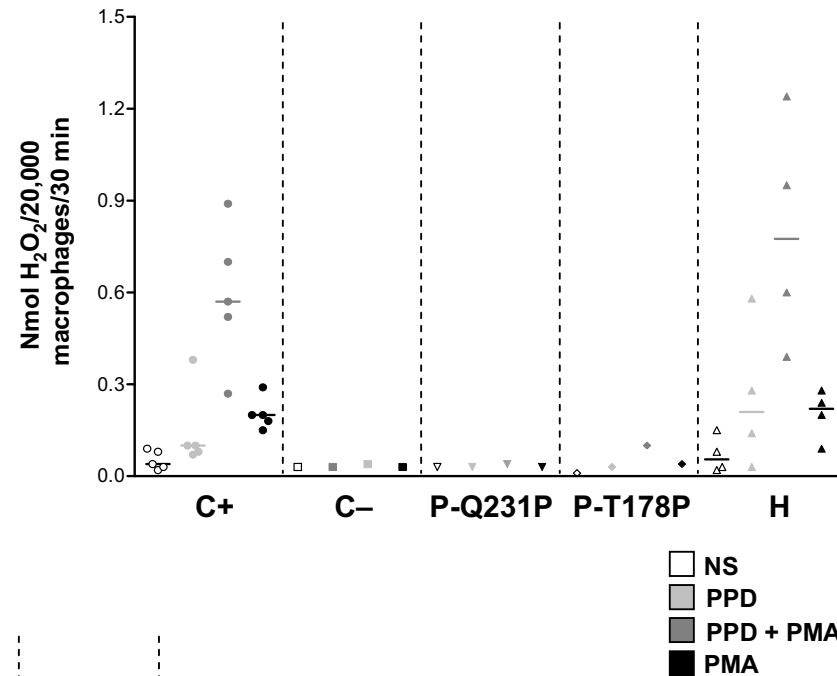
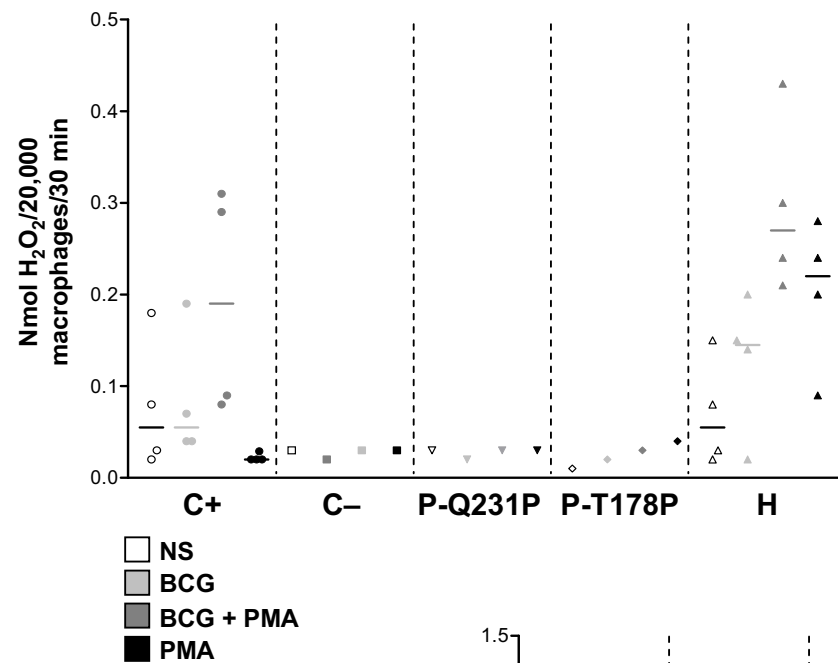
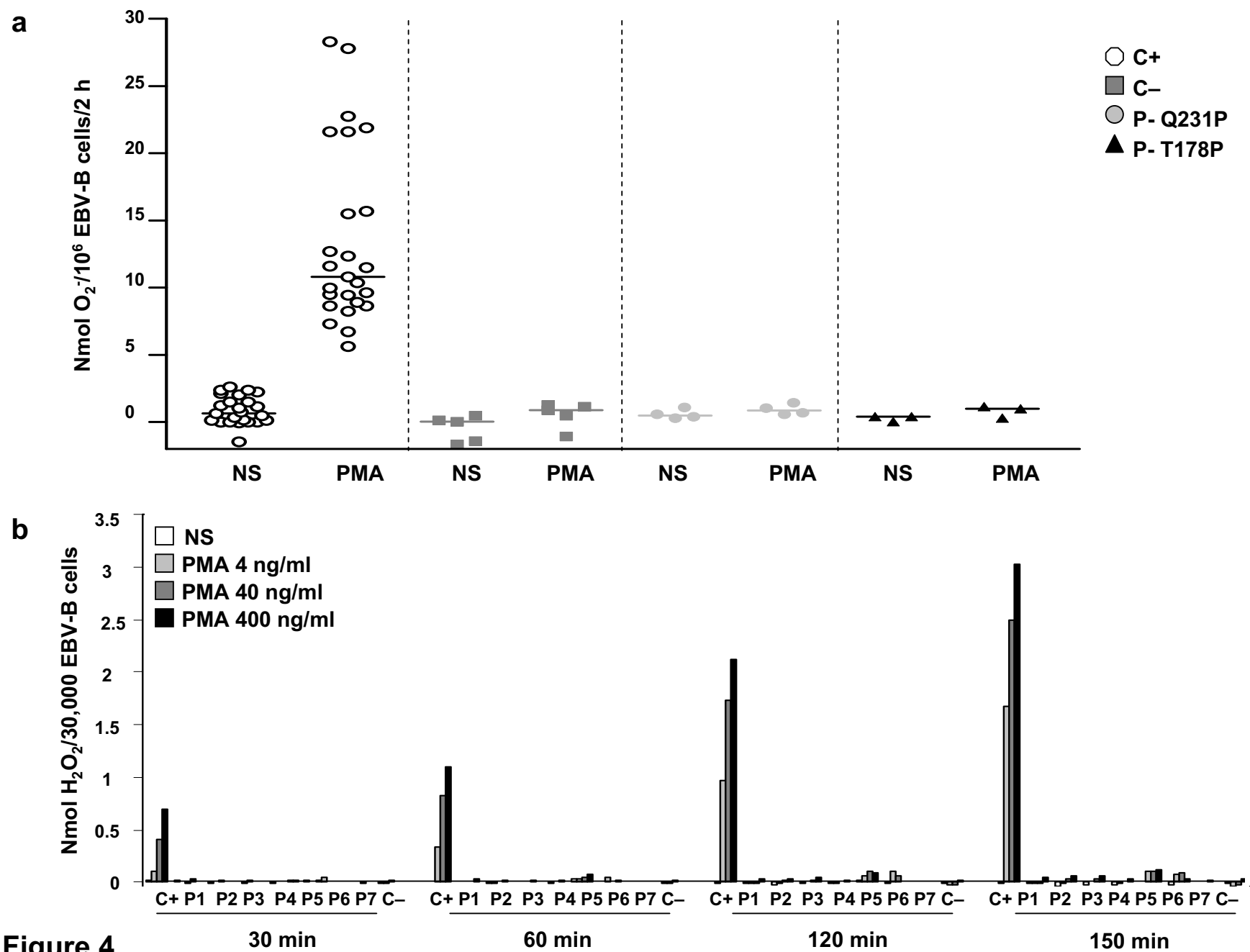
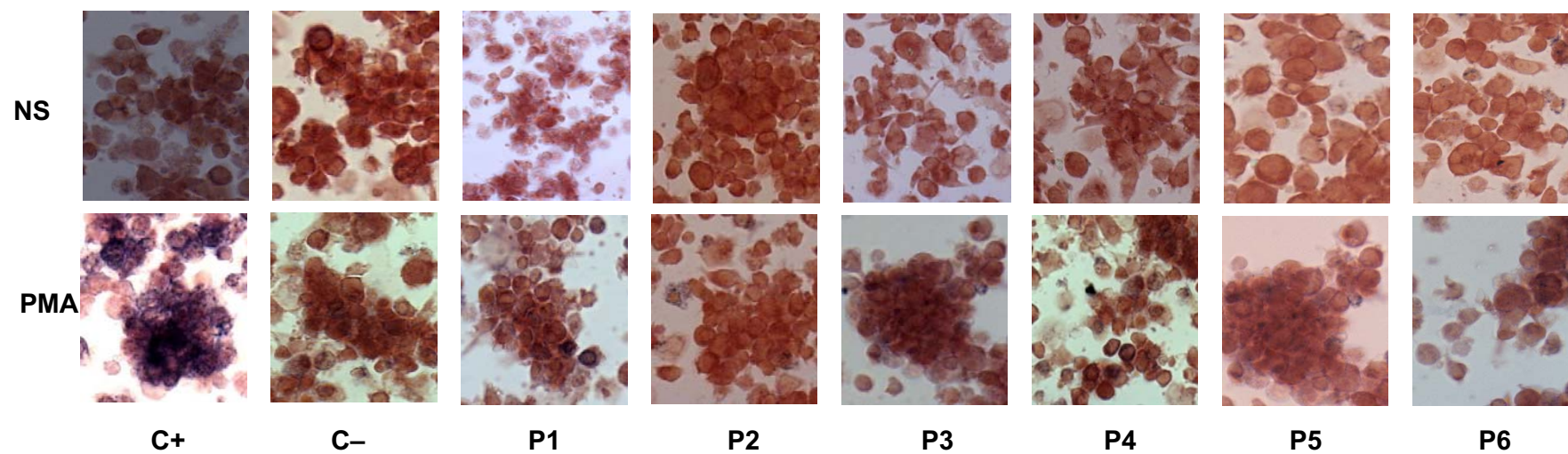
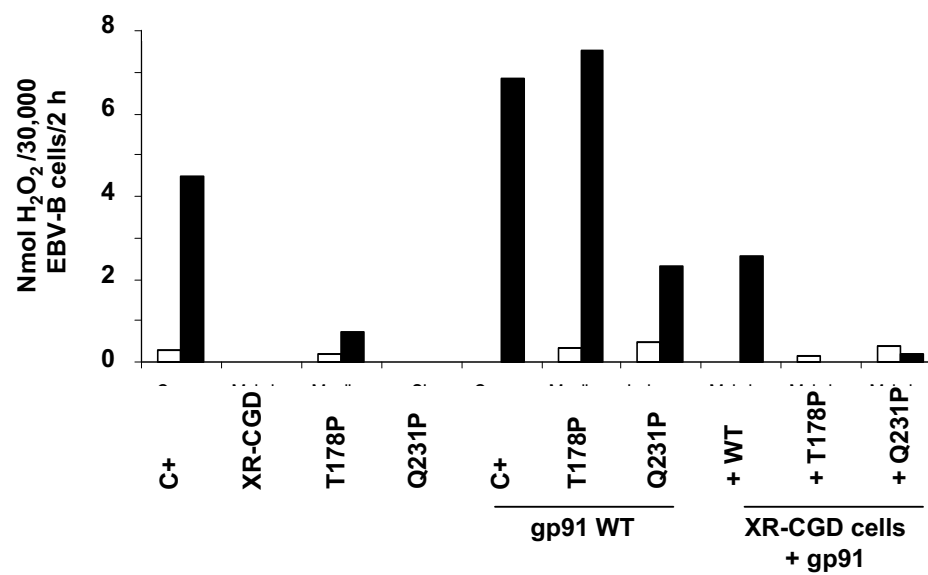


Figure 3



**Figure 4**

**c****d****Figure 4**

**a**

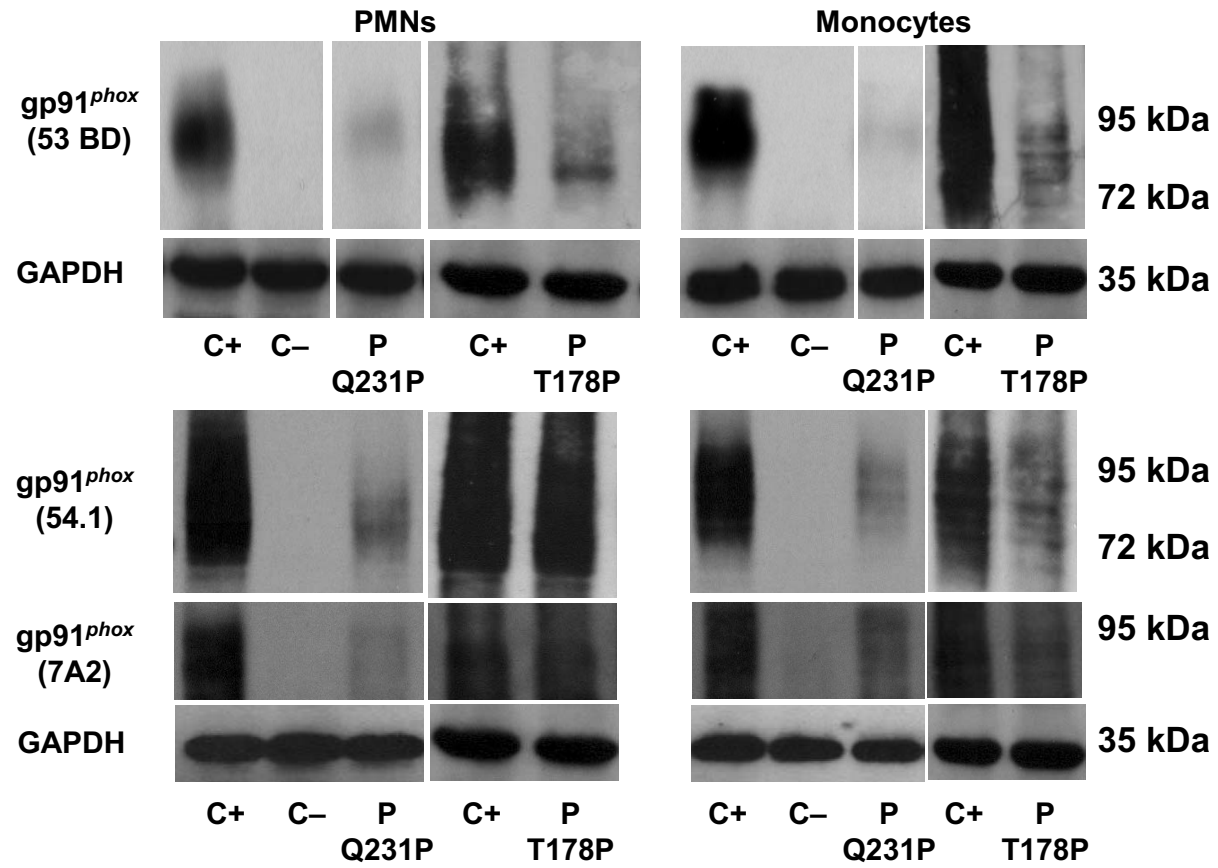


**Figure 5**

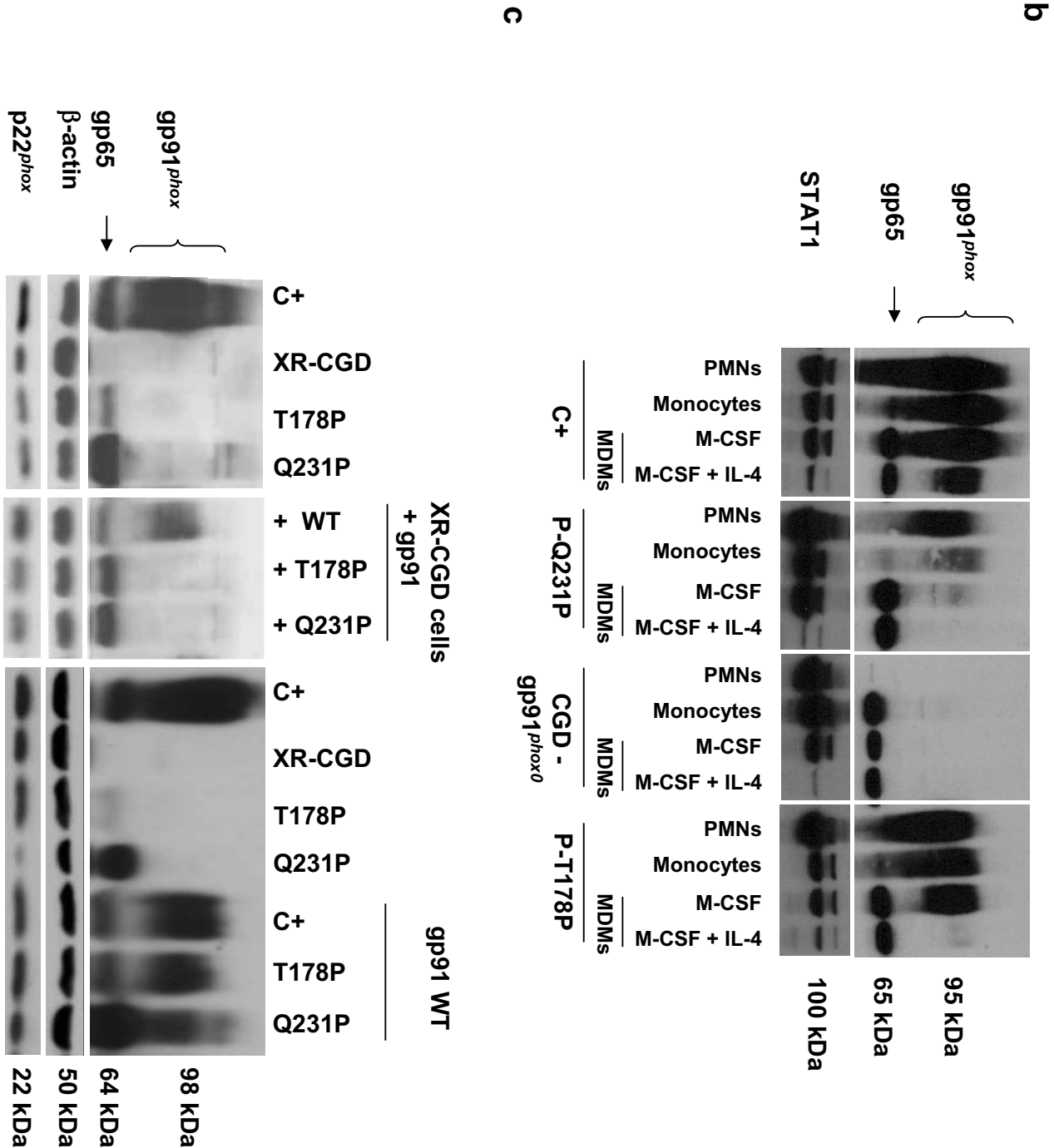
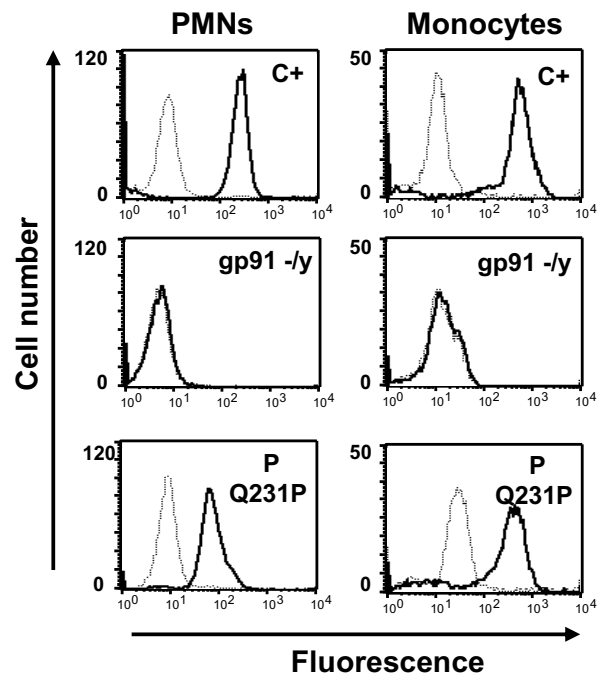
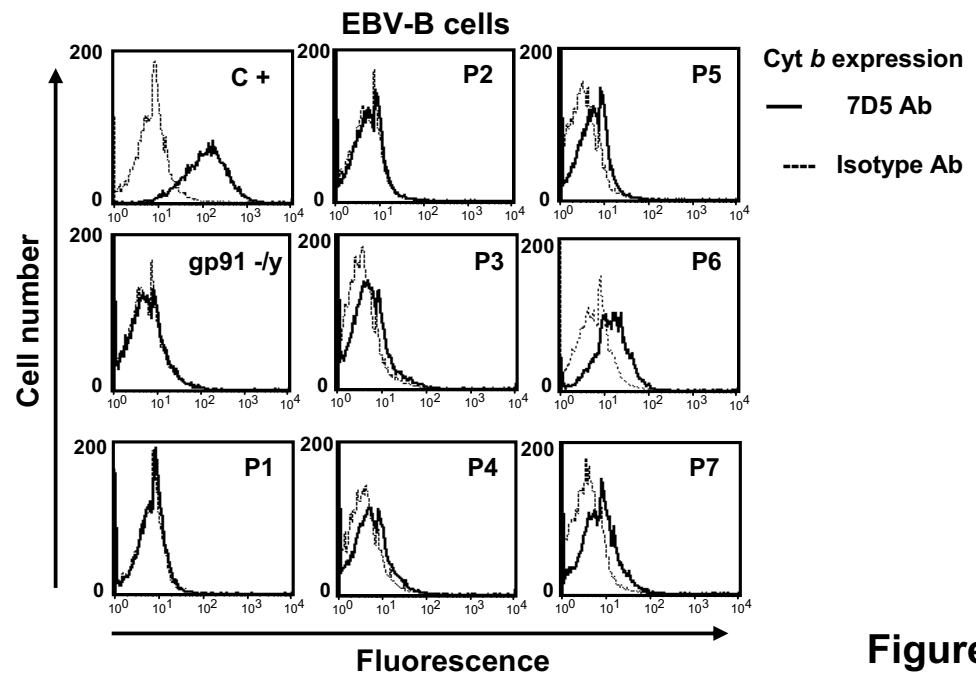
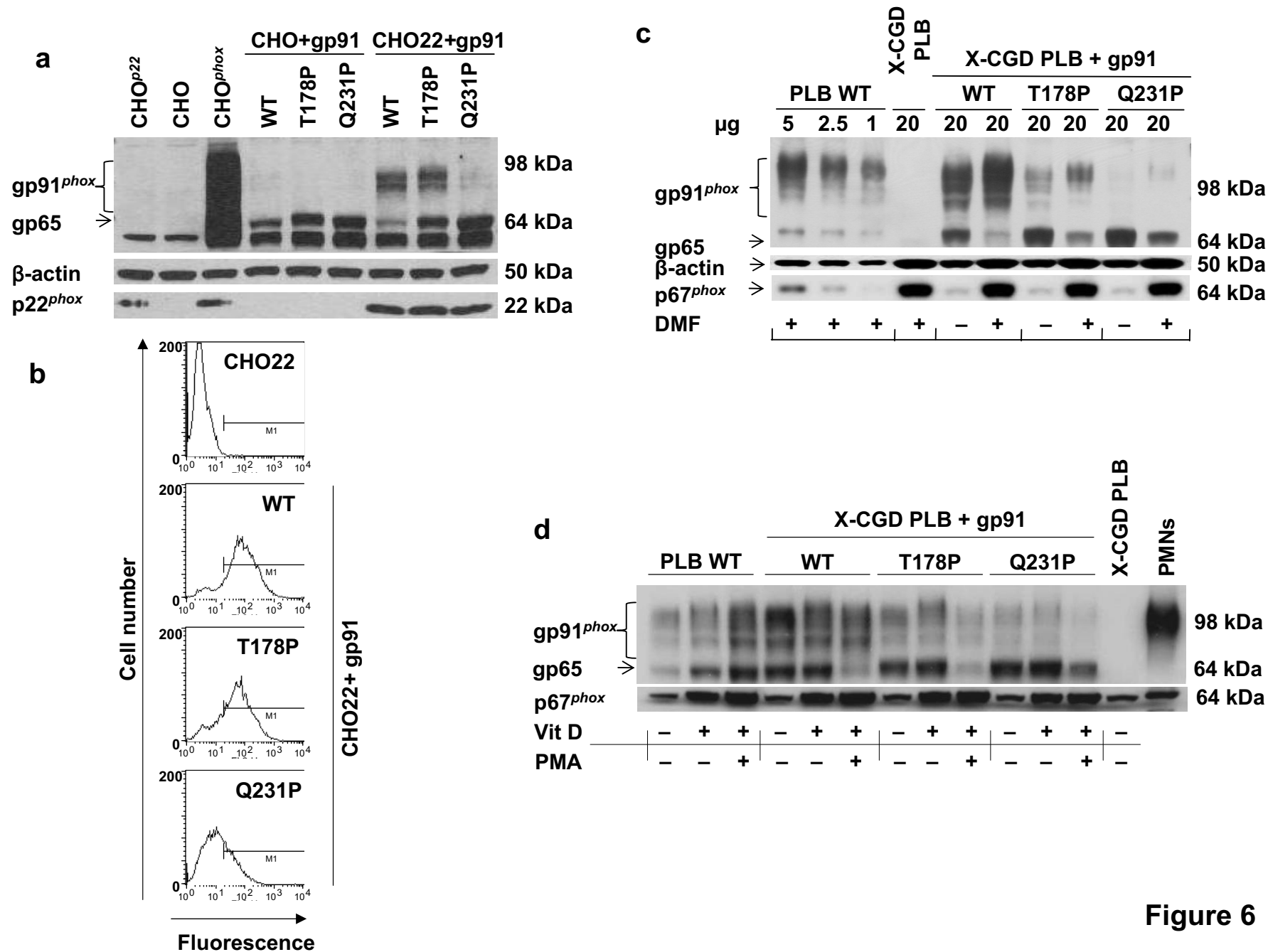


Figure 5

**d****e****Figure 5**



**Figure 6**